3-22-2017

Combinatorial efficacy of antimicrobial peptides and silver ions

Christina Lynne Chrom
Rowan University

COMBINATORIAL EFFICACY OF ANTIMICROBIAL PEPTIDES AND SILVER IONS

by

Christina L. Chrom

A Thesis

Submitted to the
Department of Chemistry & Biochemistry
College of Science and Mathematics
In partial fulfillment of the requirement
For the degree of
Master of Science in Pharmaceutical Sciences
at
Rowan University
February 2, 2017

Thesis Chair: Gregory A. Caputo, Ph.D.

Dedication

This paper is dedicated to my parents Linda and Kenneth who have provided with the most amazing love and support.

Acknowledgments

I would like to acknowledge my family and friends for their support throughout my educational journey. I would also like to thank my research advisor for the amount of time and effort he has committed towards teaching me and providing with so much advice throughout my years at Rowan. He has truly been a great mentor and friend.

Abstract

Christina L. Chrom
COMBINATORIAL EFFICACY OF ANTIMICROBIAL PEPTIDES AND SILVER IONS
2016-2017
Gregory A. Caputo, Ph.D.
Master of Science in Pharmaceutical Science

Antimicrobial peptides are produced by multicellular organisms as a defense against competing pathogenic microbes. The mechanism of action for positively charged antimicrobial peptides is widely believed to occur when the positively charged peptide interacts with the negatively charged outer lipid membrane followed by the insertion of the peptide into the membrane. This insertion into the outer or cytoplasmic membranes leads to disruption of membrane integrity. Alternatively, silver based antimicrobials, which have been well known for centuries, are thought to act by inhibiting the proton motive force, the respiratory electron transport chain, and by affecting membrane permeability resulting in cell death. Considering the different proposed modes of action, we investigated the combination of these two antimicrobial species in an attempt to enhance efficacy by targeting different cellular processes. We performed biophysical and microbiological characterization using fluorescence spectroscopy, circular dichroism (CD) spectroscopy, vesicle permeabilization assays, bacterial permeabilization assays, and minimal inhibitory concentration (MIC) assays. While all five peptides tested in this study exhibited binding to model lipid membranes, the truncated peptides showed no measurable antimicrobial activity. The most active peptide proved to be the parent peptide AP3 with the highest degree of leakage and bacterial membrane permeabilization.

Moreover it was found that the ability to permeabilize model and bacterial membranes correlated most closely with the ability to predict antimicrobial activity. The mechanism of enhancement is under investigation along with expansion to other strains and various other antimicrobial peptides. Combinatorial delivery of antimicrobials with different sizes and modes of action appears to be a promising approach while minimizing potent toxicity and resistance concerns.

Table of Contents

Abstract v

List of Figures x

List of Tables xii

Chapter 1: Overview of Antimicrobials 1

Background 1

History of Antimicrobials 1

Early and Present Uses of Silver as an Antimicrobial 2

Silver Resistance in Bacteria 3

Antimicrobial Peptides Used as an Antimicrobial Agent 4

Mechanism of Action of Cationic Antimicrobial Peptides 5

Antimicrobial Peptides Derived from Venoms and Toxins. 6

Cationic Antimicrobial Peptide Decoralin. 6

Cationic Antimicrobial Peptide AP3 7

Introduction of Synergy as a Solution to Antibiotic Resistant Bacteria. 7

Chapter 2: Characterization and Antimicrobial Activity of Amphiphilic Peptide AP3 and Derivative Sequences 11

Introduction 11

Materials and Methods 14

Peptide Preparation 14

Bacterial Culturing 14

Minimum Inhibitory Assay (MIC) 15

Lipid Preparation 15

Binding Experiments 16

Table of Contents (continued)

Acrylamide Quenching....16

Circular Dichroism....16

Calcein Leakage Assay....16

Bacterial Outer Membrane Permeabilization Assay....17

Bacterial Inner Membrane Permeabilization Assay....18

Measurement of Cell Viability....18

Results....19

Minimum Inhibitory Concentration (MIC)....19

Lipid Binding....22

Fluorescence Quenching.....25

Circular Dichroism....28

Calcein Leakage....30

Bacterial Membrane Permeabilization....33

Mammalian Cell Viability....38

Discussion....39

Conclusions....43

Chapter 3: Characterization, Antimicrobial and Synergistic Effect of Decoralin and Silver Nitrate....47

Introduction....47

Material and Methods....48

Bacterial Culturing....48

Minimum Inhibitory Assay (MIC)....48

Lipid Preparation....48

Table of Contents (continued)

Binding Experiments 48

Acrylamide Quenching 48

Circular Dichroism 48

Calcein Leakage Assay 48

Bacterial Outer Membrane Permeabilization Assay 48

Bacterial Inner Membrane Permeabilization Assay 48

Bacterial Growth Analysis 48

Synergy assay 49

Results 49

Lipid Binding 49

Fluorescence Quenching 51

Circular Dichroism 52

Calcein Leakage 54

Bacterial Membrane Permeabilization 56

Antibacterial Activity 59

Discussion 66

References 70

List of Figures

Figure Page

Figure 1. Superbugs vs. Spiders....8

Figure 2. Solitary Eumenine Wasp, Oreumenes decoratus....9

Figure 3. Winter Flounder Pleuronectes americanus....9

Figure 4. Schematic of Peptide Pore Formation....10

Figure 5. Helical Wheels of (A) AP3 and Derivative Sequences (B)AP3K, (C)APX, (D)APX-17, and (E)APX-12. 13

Figure 6. Peptide Binding to Lipid Vesicles....23

Figure 7. Peptide Binding to Lipid Vesicles by Spectral Shifts 24

Figure 8. Barycenter Shift....25

Figure 9. Fluorescence Quenching 27

Figure 10. Circular Dichroism 29

Figure 11. Vesicle Leakage Assay....31

Figure 12. Calcein Leakage as a Function of Peptide/Lipid Concentration 32

Figure 13. Outer-Membrane Permeability-Full Time Course 34

Figure 14. Outer-Membrane Permeability....35

Figure 15. Inner-Membrane Permeability-Full Time Course....37

Figure 16. Inner-Membrane Permeability....38

Figure 17. MTT Assay....39

Figure 18. Decoralin Binding to Lipid Vesicles by Spectral Shifts....50

Figure 19. Barycenter Shift of Decoralin....51

Figure 20. Fluorescence Quenching of Decoralin 52

Figure 21. Circular Dichroism of Decoralin....53

List of Figures (continued)

Figure 22. Vesicle Leakage Assay of Decoralin and L1 55

Figure 23. Outer-Membrane Permeability of E. coli With Decoralin 57

Figure 24. Inner-Membrane Permeability of E. coli With Decoralin 58

Figure 25. Kinetics of E. coli and S. Aureus With Decoralin.....62

Figure 26. Synergy of Decoralin and Silver Nitrate 64

Figure 27. Synergy of L1 and Silver Nitrate.....65

List of Tables

Table Page

Table 1. Peptide Sequences....12

Table 2. MIC (μM) for S. aureus, E. coli P. aeruginosa, and K. pneumonia....20

Table 3. Combinatorial MIC (μM) for S. aureus, E. coli, P. aeruginosa and K. pneumonia with AP3....20

Table 4. Combinatorial MIC (μM) for S. aureus, E. coli, P. aeruginosa and K. pneumonia with AP3K....21

Table 5. Combinatorial MIC (μM) for S. aureus, E. coli, P. aeruginosa and K. pneumonia with APX....21

Table 6. Overview of Results for AP Peptides....44

Table 7. Overview of Leakage and Permeabilization Results for AP Peptides....46

Table 8. Combinatorial MIC (μM) for S. aureus, E. coli, P. aeruginosa and K. pneumonia with Decoralin....60

Table 9. Combinatorial MIC (μM) for S. aureus, E. coli, P. aeruginosa and K. pneumonia with L1....61

Table 10. APX-12 and Decoralin Comparison....68

Chapter 1

Overview of Antimicrobials

Background

History of antimicrobials. Since ancient history, natural products were often used as a means of treating a variety of human conditions and earliest records include using natural derived compounds for specific health conditions. This included using a variety of natural sources and remedies for bacterial infections, which at the time were not previous known to be caused by bacteria. Consistent with this, natural products have been and continue to be a major source of drug discovery, especially for antibiotics[1, 2]. The golden age of antibiotics began in 1930s with the discovery and development of penicillin, a natural product, by Alexander Fleming[2, 3]. Shortly after this development other common antibiotics, including streptomycin, chloramphenicol and tetracycline, emerged[3]. The majority of antibiotics that are still in clinical use were discovered between 1940 to 1980 and are natural products or natural product-derived compounds[1].

Antibiotics are one of the most commonly prescribed classes of drug but around 50% are considered to be unnecessarily prescribed or others are not given the appropriate treatment[4, 5]. This overuse and misuse has contributed to the global problem of antibiotic resistance[4-6]. There are more than 70% of pathogenic bacteria are resistant to at least one antibiotic that is currently on the market[7, 8]. Antibiotic resistant bacteria have been isolated from both hospital and community settings where they have caused serious life-threatening illnesses[9]. As a direct result of these antibiotic resistant bacteria around 23,000 deaths occur per year (Figure 1). If this global crisis continues to increase,

and if actions are not taken to decrease the ongoing problem, the world might return to a preantibiotic-era in which common infections may become severe[8] [10].

There are several ways that bacteria develop resistance including genetic mutation and modification of existing or new genetic material[6]. Resistant strains therefore have a competitive advantage in an infection when antibiotics are prescribed[5]. After the development of resistance, bacteria can then pass the resistance genes to its progeny or other bacteria[6, 11]. This transfer can occur through bacteriophage-mediated transfer of DNA, DNA taken up from the external environment or DNA transfer by cell-to-cell contact[6]. Bacterial biofilms are another method by which bacteria can become resistant to antibiotic[9]. Biofilms formation occurs through the adhesion of bacteria to a surface which leads to colonization of bacteria in a matrix of extracellular polymeric substances[12, 13]. This biofilm formation is able to protect the microorganism against antibiotics that would normally eliminate the much less dense planktonic cell[9, 12]. It is believed that 60% of bacterial infections and up to 80% of chronic infections occur as a result of bacterial growth within biofilms[14, 15]. Because of this increasing problem of resistance for antibiotics and other antimicrobial it has become critical to try and discovery new strategies for antimicrobial treatments.

Early and present uses of silver as an antimicrobial. Historical evidence shows that silver has been used as early 4,000 B.C.E. in health and medicine[16]. These include blood purification, treatment of skin ulcers, and preservation of food and water[16]. Until the wide spread development of antibiotics in the 1940s, electric colloids of silver were used as the foundation of antimicrobial therapy[16]. Within recent years, antibiotic-resistant bacteria have proliferated necessitating the development of alternative strategies

to combat infection caused by these resistant bacteria[17, 18]. Silver has been found to be one class of molecules that have a low propensity for resistance development. The long-standing application of silver as an antimicrobial, combined with the antibiotic resistance bacteria has the investigation as a potential tool or component of combinatorial therapies to address this emerging threat. Recent reports describe silver being used for skin ulcer treatment, wound treatment, dental hygiene, catheters and compound fracture[16, 18, 19].

There are various formulations and delivery routes for biomedical applications of silver. However it is widely believed that the ionic form (Ag^+) is known to be responsible for the antimicrobial activity. However there is still no definitive mechanism of action for the antimicrobial activity of Ag^+. Several proposed mechanisms that are thought to be responsible for the antimicrobial activity including enzyme deactivation through thiol reactivity, disruption of the electron transport chain, cell membrane disruption, interaction with bacterial cell DNA, and destruction of bacterial cells by free-radicals[19, 20].

Silver resistance in bacteria. With silver being used throughout history, there have been some reports of silver resistance development in bacteria. These resistant bacterial strains have been isolated in hospital settings[21],[22]. There are several genes carried on bacterial plasmids responsible for resistance to silver[21]. The molecular mechanism of resistance involves a periplasmic metal-binding protein, a chemiosmotic efflux pump and ATPase efflux pump[23]. These plasmid-encoded pumps, which actively transfer the Ag^+ out of the cell, are thought to be a major sources of the silver resistance[23],[24]. The development of silver resistance is not very widespread which can be attributed to the broad-spectrum activity and the proposed mechanisms of action,

which target multiple bacterial components[25]. Although resistance to silver can develop, the rate of development appears to be slower than for other antimicrobial agents, which still gives promise to future development of silver based antimicrobial therapies[22].

Antimicrobial peptides used as an antimicrobial agent. Another class of molecules that have low propensity for resistance is antimicrobial peptides (AMPs). Antimicrobial peptides are biomolecules that have been conserved through evolution and are found in all complex living organisms[26],[27]. There is significant diversity in peptides that exhibit antimicrobial activity. One of the most well studied classes are those which are ribosomally synthesized as part of the natural host defense mechanism[28],[29],[30] . AMPs are widely used as a defense mechanism in multicellular organisms and are often produced to play an important role in innate immune systems and the host defense mechanism[31],[32],[33],[34]. As such, bacteria have been exposed to AMPs throughout millions of years of evolution yet there has not been any significant development of resistance[35]. This low propensity for resistance and ability to kill or inhibit bacterial growth has made AMPs an ideal target for new drug discovery to help combat antibiotic resistant bacteria[26],[35].

Naturally occurring antimicrobial peptides are gene-encoded, ribosomally synthesized polypeptides[36]. These peptides are usually short (fewer than 100 amino acid residues), have a positive net charge, amphipathic nature, and often exhibit a broad spectrum of activity against bacteria, viruses and fungi[26],[37],[38]. Because of the wide sequence and structural diversity, AMPs are traditionally classified based on secondary structure conformations: α-helices, β-sheets or random coils[26]. There are several well-

known examples of antimicrobial peptides belonging to the families of the cathelicidins[31] and defensins[31], both of which are derived from vertebrates and invertebrates. Other examples include plant-derived thionins[39], insect-derived cecropins[40] and amphibian-derived magainins[41].

Mechanism of action of cationic antimicrobial peptides. The mechanism of action for cationic antimicrobial peptides isn't fully understood. The majority of hypotheses on the mechanism of action begin with the positively charged peptide interacting with negatively charged bacterial cell surface[26],[35],[37]. This interaction is followed by the insertion of the peptide into the membrane leading to disruption of the lipid bilayer. This process is thought to be driven by the partitioning of hydrophobic amino acid side chains in the nonpolar core of the bacterial membrane. While it is difficult to investigate in bacterial systems, using model membrane vesicles approaches, the binding and insertion of the AMPs into the bilayer is often concomitant with secondary structure rearrangement in the peptide.

There are several physical models that have been proposed for the membrane disruptive activity of AMPs. The barrel stave model involves the insertion of the peptide into the membrane which forms a purely proteinaceous pore[42]. In the toroidal pore model, AMPs cause bending of the lipid membrane leading to the formation of a protein and lipid headgroup-lined pore. In the carpet model AMPs cause destabilization of the cell membrane through a mass action effect similar to a micellization type mechanism[43].

Antimicrobial peptides derived from venoms and toxins. While many antimicrobial peptides are naturally occurring components of the innate immune system of higher organisms, other naturally occurring peptides can also exhibit antimicrobial activity. Naturally occurring venoms and toxins often contain a cocktail of biologically active molecules and have been a rich source for the identification of antimicrobial peptides. Many of these peptides function naturally to damage cell membranes as part of the mechanism of action of the venom. Animal venoms and toxins have an evolutionary pressure to increase its defense and ability to improve prey capture[44]. Due to this diversity, peptides from naturally occurring venoms and toxins have become an area of interest because they interact with a wide variety of molecular targets.[44] Well-characterized examples include the honeybee venom peptides melittin[45], wasp peptides MP1 and mastoparan, and the rattlesnake toxin crotamine[46].

Cationic antimicrobial peptide decoralin. Venomous arthropods often produce venom mixtures that include peptides with antimicrobial activity. These complex venoms are naturally used to suppress prey[47]. The venom of the solitary eumenine wasp, *Oreumenes decoratus* (Figure 2) is a mixture that includes an 11 residue peptide with is commonly referred to as decoralin[33]. Decoralin has been characterized as a linear, cationic alpha-helical peptide consisting of hydrophobic and basic amino acids[33]. Synthetic analogs of the original decoralin sequence have been characterized and the biological activities investigated. In a study preformed by Konno et al., the C-terminus of decoralin was amidated, resulting in higher levels of helicity and decreased hemolytic activity when compared to the original sequence[33]. The amidated analog of decoralin also showed greater antimicrobial activity against both Gram positive and Gram negative

bacteria[33]. These results show a great potential for decoralin analogs being a good template for new drug targets in combating antibiotic resistance.

Cationic antimicrobial peptide AP3. Antimicrobial peptides isolated from different species of fish have become a focus of research because fish abundantly express peptides as defense mechanism after hatching[48],[49]. Pleurocidins are a class of antimicrobial peptides that have been isolated from a variety of Atlantic flounder species including the winter flounder *Pleuronectes americanus* (Figure 3)[48],[50],[51]. In a study performed by Patrzkat et.al., several peptide products were isolated from the Winter flounder, including the peptide AP3. AP3 showed one of the highest antimicrobial activities of all the sequences tested and had the greatest effect on *P. aruginosa* indicted by the minimal inhibitory concentration (MIC) performed in this same study[48].

Introduction of synergy as a solution to antibiotic resistant bacteria. There are three possible combinatorial effects: additive, antagonistic, or synergistic[52]. An additive effect is one in which the effects of each agent is identical whether they are combined or singular but when combined the two effects stack[52]. An antagonistic effect is one in which the overall effect is diminished when the two entities are mixed, often through inhibition or competition[52]. Synergy is defined by two or more entities having a positive attribute when the entities are combined[53]. Therefore a synergetic effect is one in which there is a greater effect together than the individual species alone[53].

The challenge of antibiotic resistance has renewed interest in exploring combinatorial therapies using previously identified antimicrobial agents in the hope of

identifying synergistic interactions. In a study performed by Guozhi et al., two or three AMPs were combined in order determine potential synergistic effects[52]. This study found that both two-AMP and three-AMP combinations showed strong synergistic interactions[52]. These results show the promising outcome of AMPs being used in combination with other antimicrobial agents to produce a synergistic effect[52]. A similar study performed by Choi et al. tested the AMP arenicin-1 with various bacteriostatic antibiotics[54]. The study found that in almost all bacteria species tested there was a strong synergistic effect using the fractional inhibitory concentration index (FICI)[54]. These results show that the ability of bacteriostatic antibiotics and formally ineffective concentration of the peptide could be restored[54].

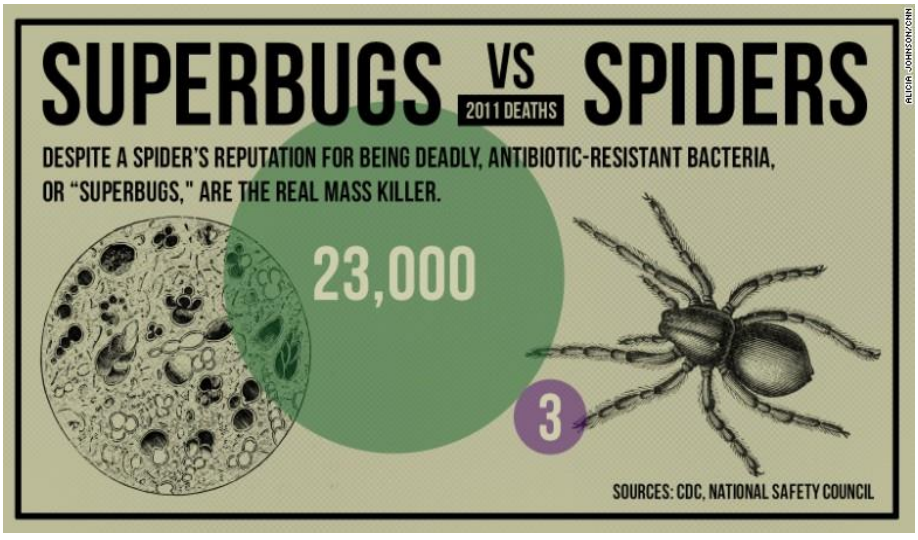

Figure 1. Superbugs vs. Spiders[55]

Figure 2. Solitary Eumenine Wasp, *Oreumenes decoratus.[56]*

Figure 3. Winter Flounder *Pleuronectes americanus.[56]*

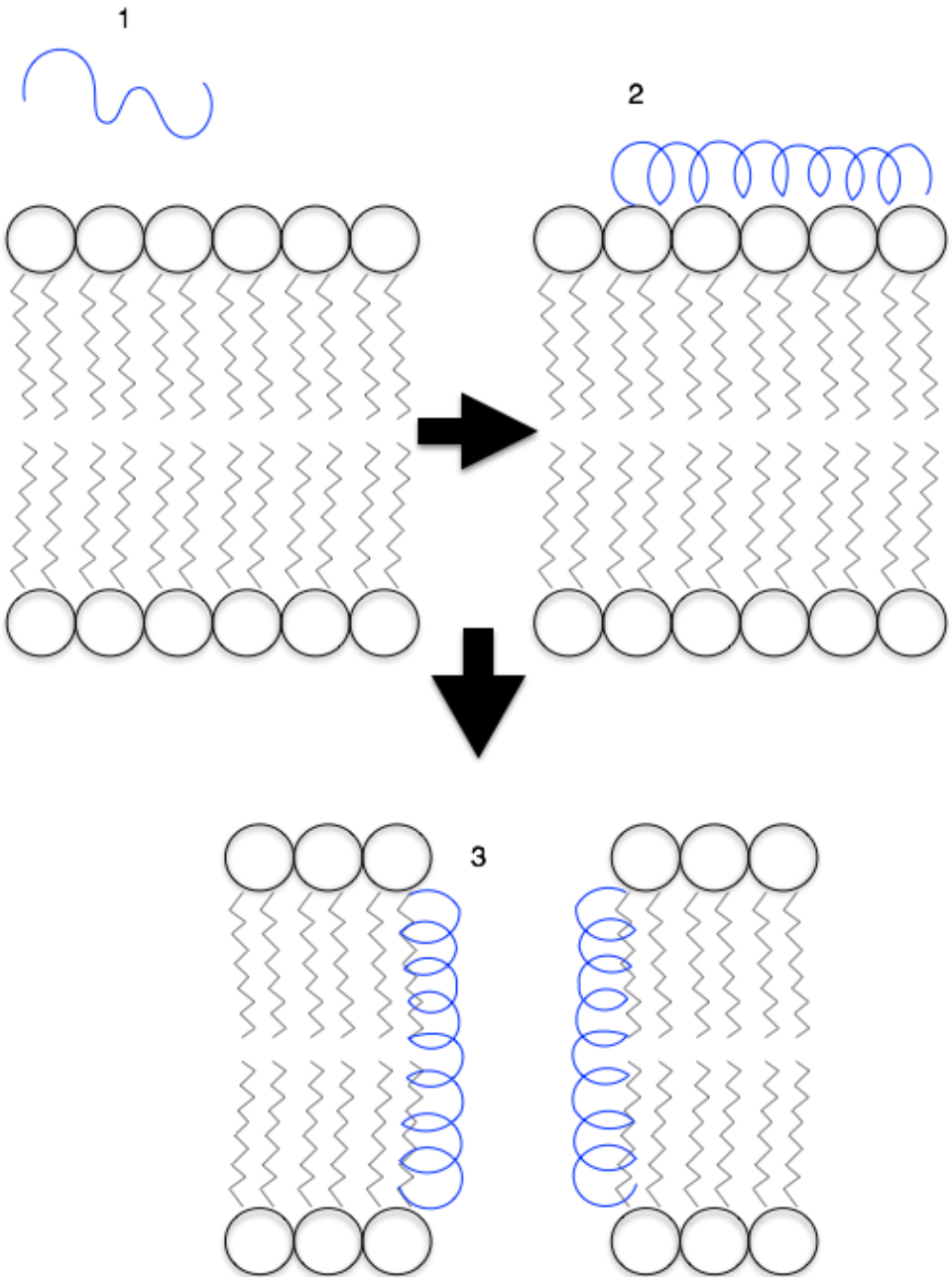

Figure 4. Schematic of Peptide Pore Formation. The schematic represents an AMP (1) transitioning from the water to the lipid bilayer, followed by (2)the peptide folding into an α-helical conformation on the surface of the bilayer. (3) The peptide then inserts into the bilayer to form a pore or other bilayer disruptive structure, therefore compromising the integrity of the membrane.

Chapter 2

Characterization and Antimicrobial Activity of Amphiphilic Peptide AP3 and Derivative Sequences

Introduction

Antimicrobial peptides isolated from different species of fish have become a focus of research because fish are abundant in peptides as defense mechanism after hatching[48],[49]. Pleurocidins are a class of antimicrobial peptides that have been isolated from a variety of Atlantic flounder species, including the winter flounder *Pleuronectes americanus*[48],[50],[51]. In this study, different analogs of the Pleurocidin like peptide AP3, from *P. americanus,* were synthesized to further investigate the sequence-structure and activity relationship in these peptides. Different analogs of AP3 were synthesized in which length, charge identity, and Trp position were varied.

Different analogs of the peptide AP3 were synthesized to further investigate the sequence-structure and activity relationship. Table 1 lists the parent and analogs peptides that were tested along with their sequences. The AP3K analog has a modified sequence that replaces the single arginine at position 3 with a lysine. This construct was synthesized to create a uniform charge and cationic functional throughout the entire peptide. The APX analog switches the position of the tyrosine normally at position 22 with the tryptophan, which is normally at position 2. This construct was designed to facilitate the incorporation of tryptophan in later constructs, as tryptophan is a good reporter in fluorescence assays and solid phase peptide synthesis proceeds from the C to N terminus. Thus allowing tryptophan to be incorporated into constructs of varied lengths. This facilitated the synthesis of truncated versions of APX consisting of either the 12 or 17 C-terminal fragments, APX-12 and APX-17 respectively. The peptides were

characterized using fluorescence spectroscopy to analyze bilayer interactions, circular dichroism to determine secondary structure, and a variety of membrane permeabilization assays.

Table 1

Peptide Sequences

		Molecular Weight			
Peptide	Sequence	Measured	Calculated[a]	Net Charge[a]	pI[a]
AP3	GWRTLLKKAEVKTVGKLALKHYL	2652.8	2653.2	+5	10.89
AP3K	GWKTLLKKAEVKTVGKLALKHYL	2617.8	2625.2	+5	10.74
APX	GYRTLLKKAEVKTVGKLALKHWL	2653.2	2653.2	+5	10.89
APX-17	KKAEVKTVGKLALKHWL	1950.2	1949.3	+4	10.85
APX-12	KTVGKLALKHWL	1393.7	1394.7	+3	10.98

a: Calculated using Innovagen Peptide property calculator http://pepcalc.com/

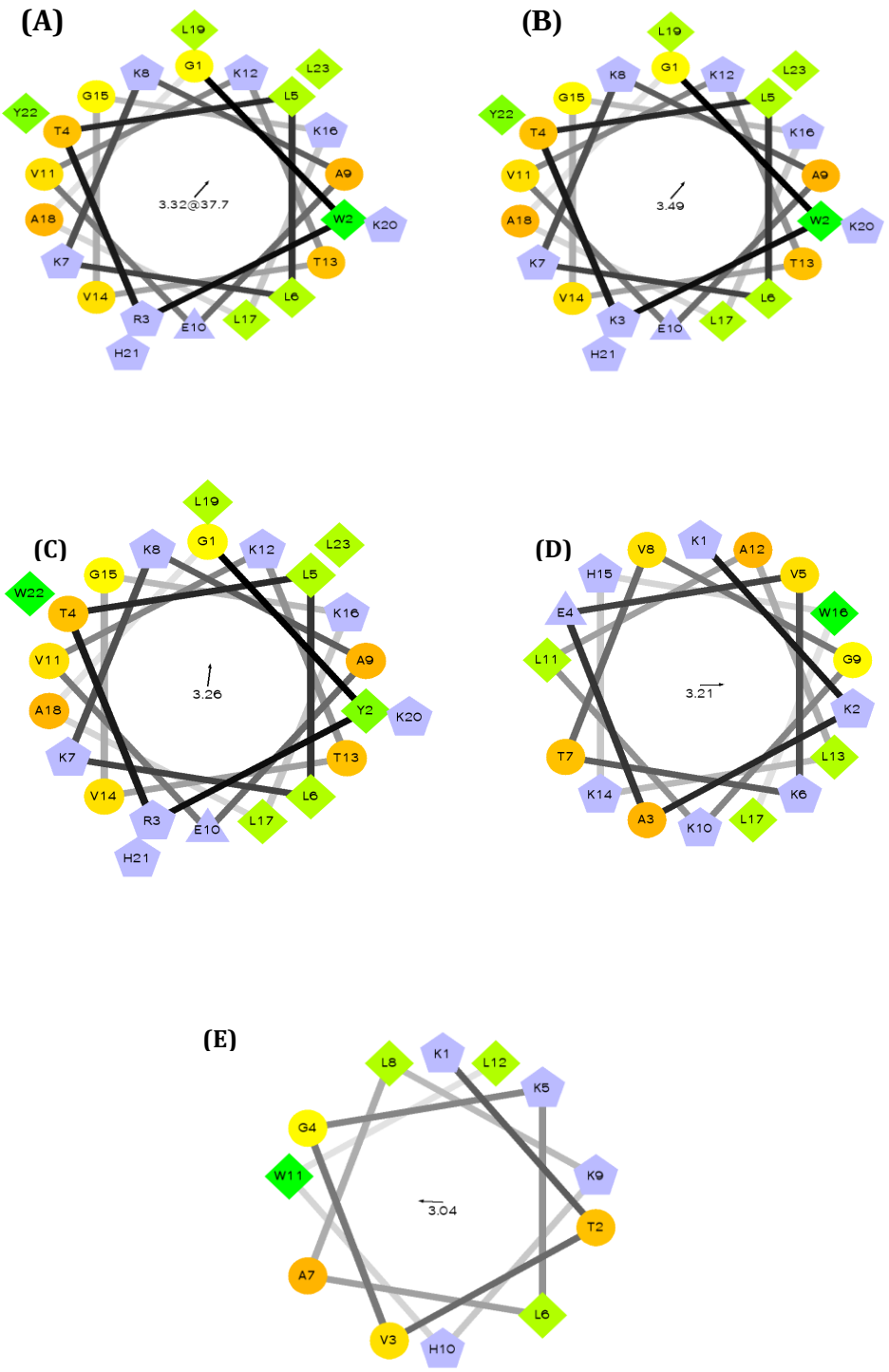

Figure 5. Helical Wheels of (A) AP3 and Derivative Sequences (B)AP3K, (C)APX, (D)APX-17, and (E)APX-12. Circles represent hydrophilic residues, diamonds as hydrophobic residues, anionic as triangles, and cationic as pentagons. Projections were made using http://rzlab.ucr.edu/scripts/wheel/wheel.cgi

Materials and Methods

Peptide preparation. The peptides APX, APX-17, and APX-12 were prepared by FMOC solid phase synthesis. Synthesis was performed on rink-amide resin using Fmoc-protected amino acids, HATU (1-[Bis(dimethylamino)methylene]-1H-1,2,3-triazolo[4,5-b]pyridinium 3-oxid hexafluorophosphate), and DIEA (*N*,*N*-Diisopropylethylamine) at a 1:1:2 ratio for couplings. Deprotections were performed using a solution of 1:4 v:v: piperidine in DMF (*N*,*N*-Dimethylformamide). Cleavage was performed by mixing the resin with a cocktail of TFA (trifluoroacetic acid):TIS (triisopropylsilane):H_2O:ETHANEDITHIOL (92.5:2.5:2.5:2.5) for ~2 h followed by filtration and peptide precipitation in cold diethyl ether. Remaining peptides were purchased from GenScript (Piscataway, NJ). All peptides were purified by reverse phase high-performance liquid chromatography using a linear gradient of solvent A (H_20 with 0.1% TFA) and solvent B (acetonitrile with 0.1% TFA). Peptides were separated on an Agilent (5 μm 9.4x250 mm) C4 column. Fractions were monitored using UV absorbance at 220 and 280 nm and peptide identity was confirmed using ESI-MS (Agilent 1100 Series LC/MSD Trap). Purified peptides were lyophilized, reconstituted in an ethanol water mixture and stored at 4 °C. Peptide stock concentration was determined spectrophotmetically as described previously.[57] [58]

Bacterial culturing. Bacteria were streaked from frozen stocks onto LB - miller agar (Difco) plates (*E. coli* MG1655 ATCC 47076, *E. coli* D31[59], *S. aureus* ATCC25923, *P. aeruginosa* ATCC10145, *K. pneumoniae* 700603). Streaked plates were grown overnight at 37 °C and subsequently stored at 4 °C.

To prepare overnight cultures, a single colony of each bacterial strain was added to LB broth (Difco) in sterile culture tubes. Tubes were placed in the shaking incubator at 37 °C overnight to allow for sufficient bacterial growth. After incubation, dilutions of the overnight culture were made in Muller-Hinton broth (Criterion) 1:100 or 1:250 for MIC (minimal inhibitory concentration) assay protocols.

Minimum inhibitory assay (MIC). Minimal inhibitory concentrations (MIC) were determined for each peptide The MIC plate was made by adding 10 μL of the peptide stock solutions to wells of a sterile 96-well plate to which 90 μL of diluted bacterial culture was added. The final bacterial load was ~5.0 x 10^5 cfu/mL as calculated from OD_{600} measurements of a log-phase culture. The assay plate was incubated at 37 °C for 18 h. Bacterial growth was assayed by absorbance at OD_{600} using Multiskan microplate reader (Thermo Fisher). The MIC was defined as the lowest peptide concentration to completely inhibit growth as judged by the absorbance at 600 nm compared to controls. All MIC values are averages of at least triplicate samples.

Lipid preparation. Stocks of POPC (1-palmitoyl-2- oleoyl-sn-glycero-3-phosphocholine) and POPG (1-palmitoyl-2- oleoyl-sn-glycero-3-phospho-(1'-rac-glycerol) (Avanti Polar Lipids) were dissolved in chloroform and stored at -20 °C. Vesicles were prepared by mixing appropriate aliquots of lipids in a glass test tube which were dried first with nitrogen gas and then under a vacuum for 1 h. Small unilamellar vesicles (SUVs) were formed by resuspending the lipid film in PBS buffer (50 mM sodium phosphate, 100 mM NaCl, pH 7.1) before sonicating in a high power bath sonicator for 18 min (Avanti Polar Lipids).

Binding experiments. Peptide binding to lipid vesicles was determined using fluorescence spectroscopy by titrating in aliquots of lipid vesicles into a sample that contained buffer and peptide. Lipid vesicles were prepared as described above with either 100% POPC (PC) or 75:25 POPC:POPG (PC:PG) lipid composition and final peptide concentration of 2 μM. Trp Emission spectra were recorded from 300 to 400 nm with an excitation of 280 nm using a Spectramax-2 spectrofluorometer (JY-Horiba, Edison NJ). All spectra were recorded at 25 °C.

Acrylamide quenching. Samples for acrylamide quenching analysis composed of 250 μM total lipid and 2 μM peptide. Samples were excited at 295 nm with emission measured over the range of 315–415 nm. Fluorescence measurements were taken prior to addition of quencher as the F_0 value. Aliquots from a 4M stock of acrylamide in water were added to the samples, mixed, and then remeasured. All spectra were recorded at 25 °C. Fluorescence from background samples containing only lipid vesicles, buffer and quenchers were subtracted. Emission intensity was also corrected for dilution by addition of the quencher and for inner filter effects by the quencher as described previously[58].

Circular dichroism. Samples were prepared in a buffer containing 1:10 diluted PBS (5 mM phosphate, 10 mM NaCl, pH 7.04) with peptide concentration of 5 μM unless specified otherwise. A Jasco J-715 CD spectrometer was used to record circular dichroism (CD) spectra using a quartz cuvette with a 1 cm path length. All spectra were recorded at 25 °C and averaged over 64 scans.

Calcein leakage assay. Lipid films were prepared as described as above for a final concentration of 20 mM (75% POPC, 25% POPG). Lipid films were rehydrated

with 46 mM calcein in 33 mM HEPES, pH 7. After being fully dissolved the sample was subjected to 11 freeze-thaw cycles by transferring between liquid nitrogen followed by 37 °C water bath. Vesicles were then extruded by passing the solution through 0.2μM polycarbonate filters for 21 passes to create large unilamellar vesicles (LUVs). Extruded LUVs were separated from free calcein using size exclusion column chromatography (Sephadex G-100). Lipid concentrations and dilution factors were determined spectroscopically using a fluorescent reporter lipid. Assays were performed in a 96 well plate was set up to such that each well contained lipid, 15 μL peptide diluted from a stock for appropriate final concentration in the wells, and HEPES buffer to a final volume of 150 μL. Complete calcein release was achieved by adding 5 μL of 170 mM Triton X-100 to each well at the end of the experiment. All data were normalized to the 100% release value according to the intensity after the Triton X-100 treatment. All experiments were performed at least in triplicate.

Bacterial outer membrane permeabilization assay. Bacterial culturing was performed as described above with the exception that *E. coli* (*E. coli* D31) was streaked onto LB-agar plates supplemented with 100 μg/mL Ampicillin. The overnight cultures and dilutions were grown in the presence of ampicillin at a final concentration of 100 μg/mL. After dilutions were grown to OD_{600} ~0.2 - 0.3, cells were then centrifuged at 2500 rpm for 15 mins and pellet was resuspended in PBS (100 mM phosphate, 200mM NaCl, pH 7.0). The permeabilization assays were carried out using a 96-well clear flat bottom plate with wells containing 10 μl of 500 μg/mL nitrocefin, 80μL of resuspended *E. coli* cell suspension, and 10 μL of peptide at various concentrations. A 0.25 mM solution of polymyxin B sulfate was used as a positive control. Immediately after

addition of peptide the nitrocefin cleavage was monitored by absorbance at 486 nm in 5 minute intervals for 1.5 h. Experiments were performed at least in triplicate.

Bacterial inner membrane permeabilization assay. Bacterial culturing was performed as mentioned above with the exception that *E. coli* (D31) was used and 50 µL of 100 mM IPTG was added to the cultures after dilution. The permeabilization assays were carried out using a 96-well clear flat bottom plate with wells containing 56.25 µL Z-buffer (100 mM Na_2HPO_4, 10 mM KCl, 1 mM $MgSO_4$, 40 mM β– mercaptoethanol, pH 7.1), 12 µL ONPG (4mg/ml), 18.75 µL *E. coli*, (5.0×10^5 cfu/ml) and 10µL of peptide or the cationic detergent CTAB as a control. After these additions the ONPG cleavage was monitored by absorbance at 420 nm in 5 minute intervals for 1.5 h. All experiments were performed at least in triplicate.

Measurement of cell viability. Cellular toxicity of specific peptides was determined by MTT ((3-(4,5-Dimethylthiazol-2-yl)-2,5-Diphenyltetrazolium Bromide)) assay. Human embryonic kidney (HEK) 293 cells with a lenti-CRE luciferase reporter gene were seeded in 96-well plates at a density of $1.5x10^4$ cells per well and incubated with 5% CO_2 at 37 °C for 24 h. Then, cells were treated with appropriate concentrations of peptides (0.0015-15µM) and control for 24 h. After treatment for 24 h, 10 µL of MTT solution (5 mg MTT/ mL PBS) was added to all wells and incubated for 4 h. Then, DMSO was added as a solubilizing agent and the absorbance was recorded at 540 nm. Each peptide concentration was performed in triplicate.

Results

Minimum inhibitory concentration (MIC). The antibacterial activities of each peptide were determined against various Gram-negative and Gram-positive bacteria using MIC assays. The MIC is defined as the lowest concentration of peptide that prevents growth of bacteria using the optical density at 600 nm under standard growth conditions[60]. The parent peptide AP3 shows equal or greater antimicrobial activity against all organisms tested when compared to the other full length and truncated analogs (Table 2). AP3 had the lowest MIC (highest activity) against *P. aeruginosa* exhibiting an MIC of approximately 0.3 μM. The AP3K variety exhibited a profile similar to the parent AP3 with no more than a two-fold difference against any strain tested. The APX variant showed very weak antimicrobial activity, only exhibiting inhibition at 16 μM for *S. aureus*. None of truncated analogs exhibited antimicrobial activity against any of the strains tested at any of the concentrations indicated.

The MIC values were then used to determine if the addition of the second antimicrobial species, silver nitrate, had any combinatorial effect on the bacteria species tested. Tables 3-5 show the MIC of each antimicrobial species alone as well as the combinatorial MIC for each full-length peptide. The combination of both silver and peptides lowered the MIC values for all bacteria species when compared to either peptide or silver nitrate alone.

Table 2

MIC (μM) for S. aureus, E. coli, P. aeruginosa, and K. pneumoniae

	S. aureus	*E. coli*	*P. aeruginosa*	*K. pneumoniae*
AP3	4.15	8.30	0.250	4.15
AP3K	2.32	9.30	0.290	>9.30
APX	16.6	>16.6	16.6	>16.6
APX-12	>15.0	>15.0	>15.0	>15.0
APX-17	>8.00	>8.00	> 8.00	>8.00

Table 3

Combinatorial MIC (μM) for S. aureus, E. coli, P. aeruginosa, and K. pneumonia with AP3

MIC (μM) for *S. aureus*, *E. coli*, *P. aeruginosa*, and *K. pneumoniae*				
	S. aureus	*E. coli*	*P. aeruginosa*	*K. pneumoniae*
AP3	4.15	8.30	0.25	4.15
Silver Nitrate	50	12.5	25	12.5
Silver Nitrate (w/Constant 2 **μM** AP3)	<1.5	<1.5	<1.5	<1.5
AP3 (w/ Constant 5 **μM** Silver Nitrate)	<0.23	<0.23	<0.23	0.46

Table 4

Combinatorial MIC (μM) for S. aureus, E. coli, P. aeruginosa, and K. pneumonia with AP3K

MIC (μM) for *S. aureus*, *E. coli*, *P. aeruginosa*, and *K. pneumoniae*				
	S. aureus	*E. coli*	*P. aeruginosa*	*K. pneumoniae*
AP3K	2.32	9.3	0.29	>9.30
Silver Nitrate	50	12.5	25	12.5
Silver Nitrate (w/Constant 2 **μM** AP3K)	<1.5	<1.5	<1.5	<1.5
AP3K (w/ Constant 5 **μM** Silver Nitrate)	<0.15	<0.15	<0.15	<0.15

Table 5

Combinatorial MIC (μM) for S. aureus, E. coli, P. aeruginosa, and K. pneumonia with APX

MIC (μM) for *S. aureus*, *E. coli*, *P. aeruginosa*, and *K. pneumoniae*				
	S. aureus	*E. coli*	*P. aeruginosa*	*K. pneumoniae*
APX	16.6	>16.60	16.6	>16.60
Silver Nitrate	50	12.5	25	12.5
Silver Nitrate (w/Constant 2 **μM** APX)	<1.5	<1.5	<1.5	<1.5
APX (w/ Constant 5 **μM** Silver Nitrate)	<0.15	<0.15	<0.15	<0.15

Lipid binding. Current understanding of antimicrobial peptide mechanism of action involves the binding of peptides to the bacterial membrane as the first step in the bactericidal activity. Binding experiments were designed to monitor the interactions of the AP peptides with model lipid bilayers. This was approached using tryptophan emission fluorescence spectroscopy due to the environmental sensitivity of tryptophan fluorescence. This sensitivity is often exploited to discriminate between the polar milieu and the more nonpolar lipid bilayer environments. Model vesicles were composed of either 100% PC or 75/25% PC/PG lipids to investigate the effect of electrostatics on the binding of peptides to bilayers. The electrostatic binding mechanism is widely accepted as a major component of the selectivity of antimicrobial peptides (bacterial membranes contain high mole fractions of anionic lipids imparting a strongly negative net charge to their cell surface)[61],[62]. However our results show that only the original parent sequence AP3 exhibited any significant shift in emission barycenter when interacting with lipid vesicles as shown in Figures 7 and 8. However peptides other than AP3 all exhibited significant changes in emission intensity upon introduction of lipid vesicles which is likely a result of binding interaction (Figure 6). Interestingly, none of the peptides in this study showed any significant preference between zwitterionic POPC vesicles and vesicles composed of 75%/25% POPC/POPG.

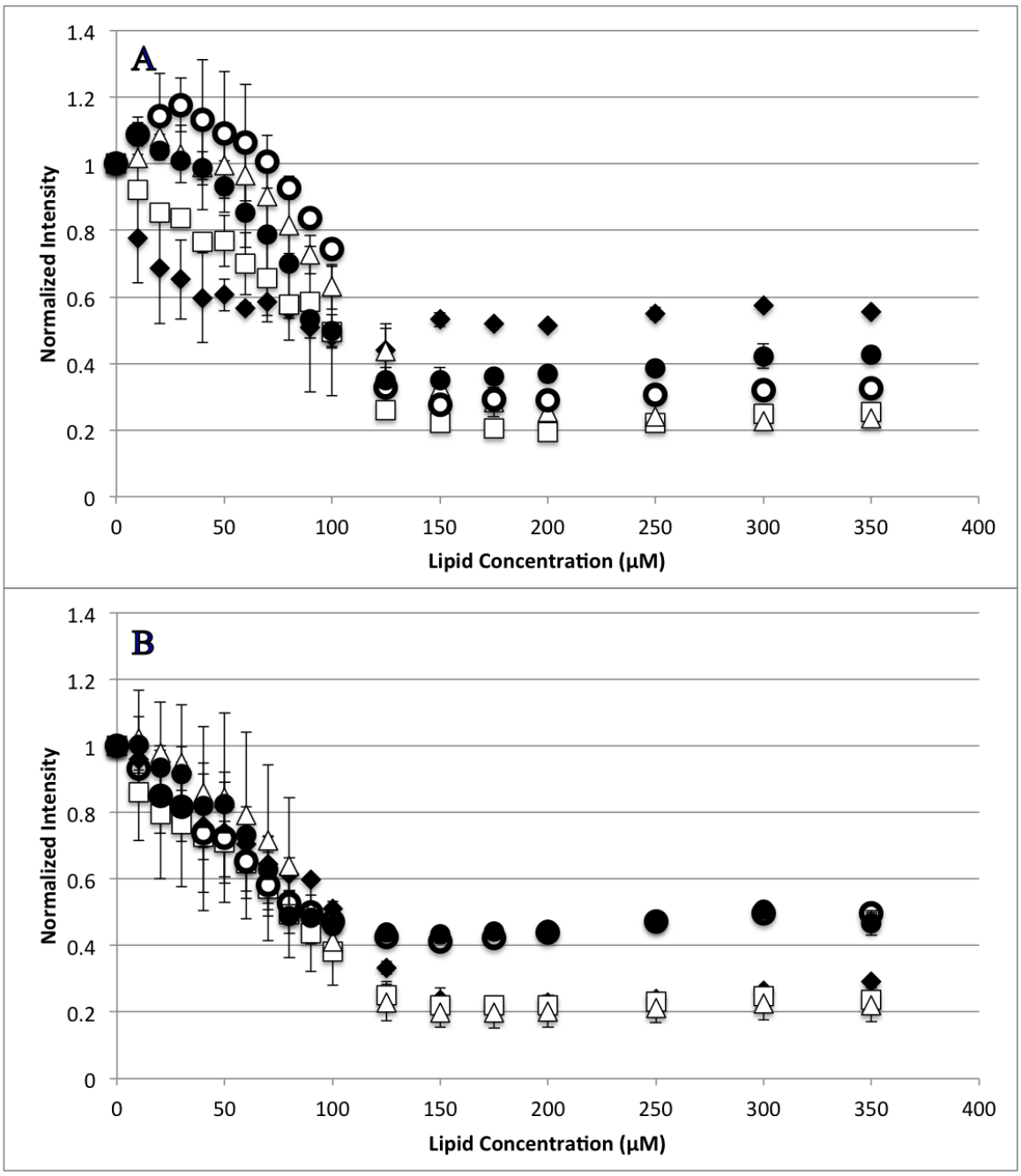

Figure 6. Peptide Binding to Lipid Vesicles. Peptide interaction with lipid vesicles was monitored using Trp emission spectra. The normalized Trp emission intensity is shown for each AP peptide titrated with either 75/25% PCPG (A) or 100% PC (B) lipid vesicles. For both graphs, AP3 is shown as diamonds (◆), AP3K as squares (■), APX as triangle (▲), APX-12 as open circle (❍), and APX-17 as closed circles (●). Peptide concentration was 2 μM in all cases. Data shown are corrected for background fluorescence and represent averages of at least three replicate samples.

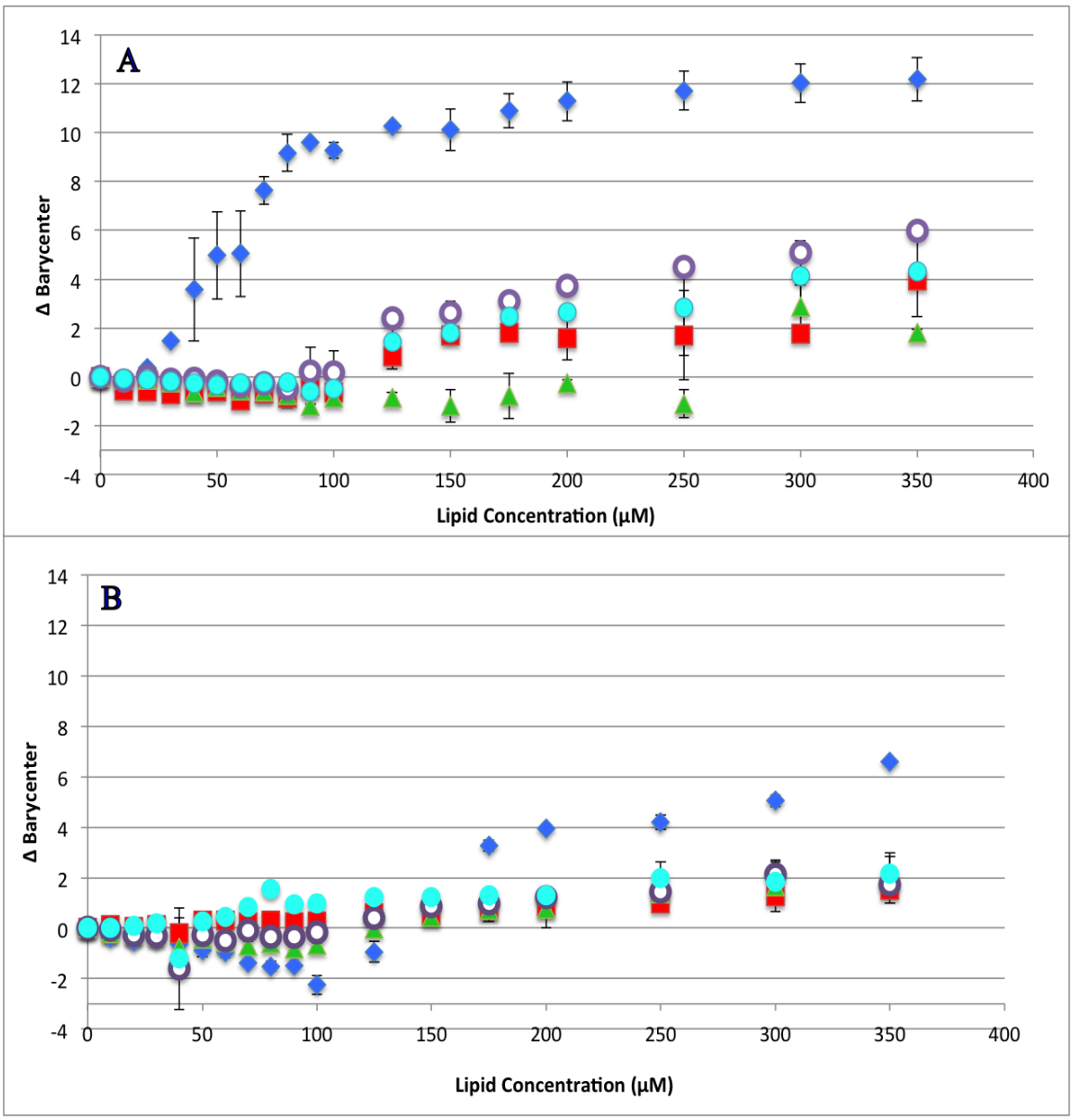

Figure 7. Peptide Binding to Lipid Vesicles by Spectral Shifts. Binding of AP peptides to lipid vesicles analyzed by change in emission spectrum barycenter as a function of lipid concentration. Each peptide was titrated with either 75:25 PC:PG (A) and 100 PC (B) vesicles. For both graphs, AP3 is shown as diamonds (◆), AP3K as squares (■), APX as triangle (▲), APX-17 as open circle (❍), and APX-12 as closed circles (●). Peptide concentration was 2 μM in all cases. Data shown are corrected for background fluorescence and represent averages of at least three replicate samples.

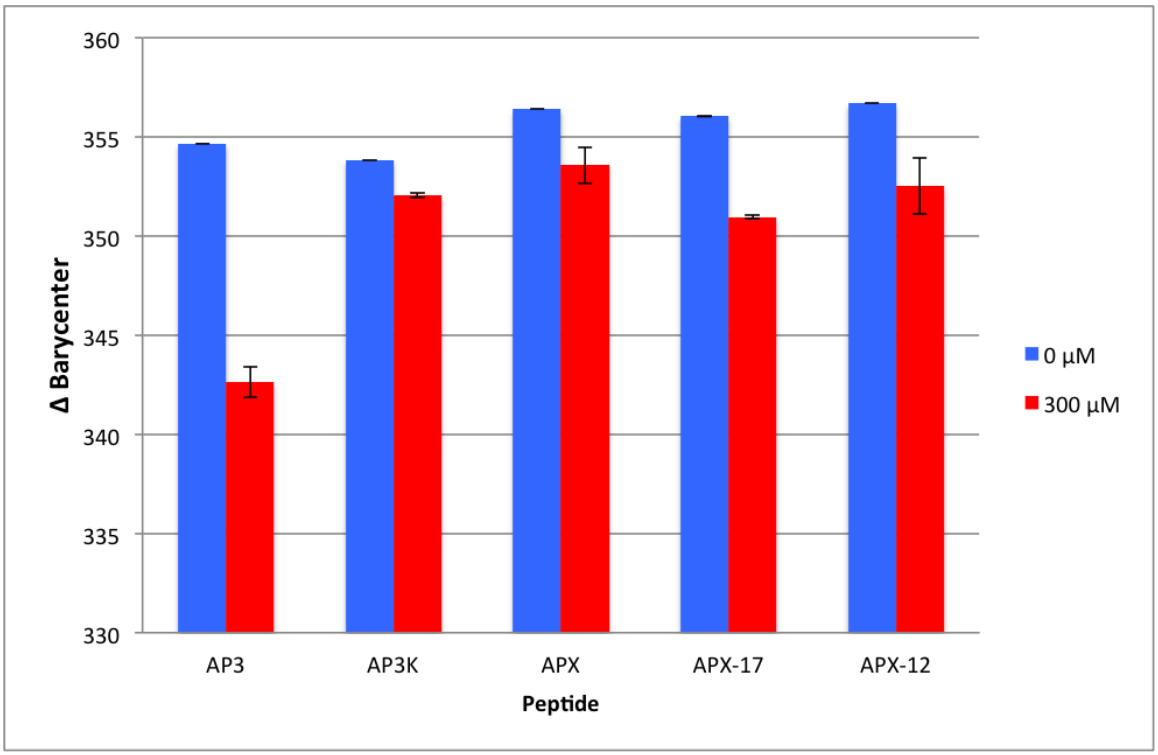

Figure 8. Barycenter Shift. Barycenter shift of AP peptides and derivatives at lipid vesicles at concentrations of 0 and 300 μM. Lipid compositions titrated were 75:25 PC:PG. Data are averages of at least three replicate samples. Parent peptide AP3 exhibits the greatest barycenter shift indicating the largest change in polarity of the local environment around Trp.

Fluorescence quenching. While the titrations described above indicate that all the peptides in this study interact with lipid membranes, the topography and structural orientation of peptides associated with the bilayer may be different among the different peptides. Changes in peptide orientation with respect to the bilayer can impact fluorescence properties as well as be related to the mechanism of action. Fluorescence quenching experiments were performed to gain insight on the origination in the bilayer. Tryptophan fluorescence quenching was performed by using the collisional quencher

acrylamide, which can strongly quench tryptophan exposed to the aqueous environments however results in very minimal quenching of tryptophan residues buried in the nonpolar core of the bilayer[58],[63]. Quenching of the peptides were compared in the presence and absence of lipid vesicles. For the full length peptides, AP3 and APX were more strongly quenched in the absence of lipid compared to presence of lipid, indicating a greater degree of occlusion of the tryptophan when bound to the lipid bilayer (Figure 9). Interestingly the AP3K peptide showed very little difference in quenching profile with and without lipid indicating that the AP3K peptide may adopt a different 3D topography when bound to the bilayer compared to AP3 and APX (Figure 9). Truncated analogs of APX show similar results to AP3K in that there was no significant difference in quenching between the bound and unbound samples. This is indicative that, when bound, the AP3K and the truncated analogs adopt a structure that orients the tryptophan more shallowly in the bilayer increasing the exposure to acrylamide in the aqueous environment.

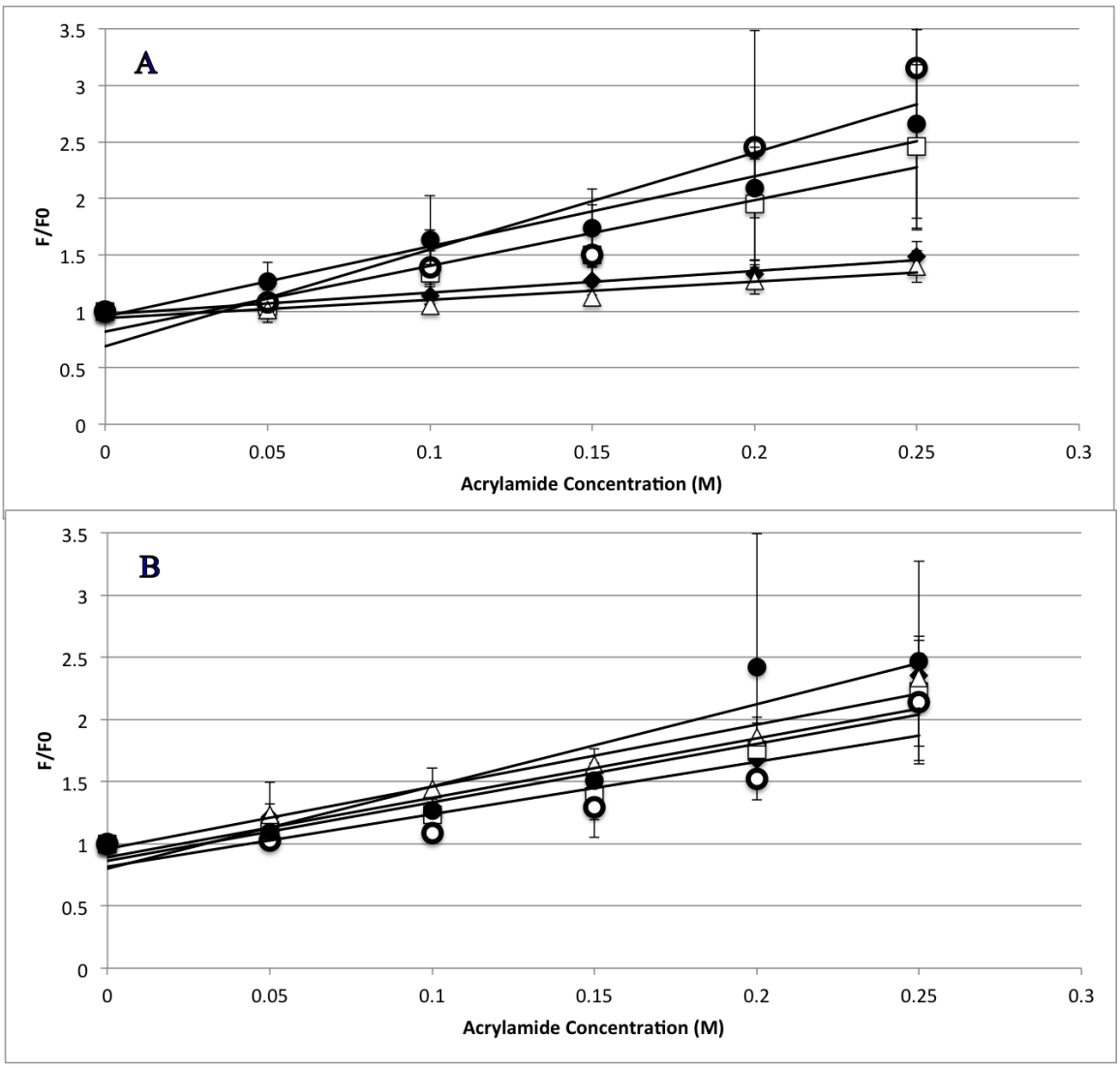

Figure 9. Fluorescence Quenching. Fluorescence quenching of AP3 and derivatives by acrylamide in the presence (A) or absence (B) of lipid vesicles. For both graphs, AP3 is shown as diamonds (◆), AP3K as squares (■), APX as triangle (▲), APX-17 as open circle (❍), and APX-12 as closed circles (●). Quenching of 2 μM peptide at pH 7 is shown in the presence of 75:25% POPC:POPG vesicles and100% POPC vesicles both totaling a final concentration of 250 μM. Data shown are corrected for background fluorescence, inner filter effects, and are averages of at least three replicate samples.

Circular dichroism. CD spectra were collected for peptides dissolved in pH 7 buffer, pH 7 buffer with lipid vesicles (75/25% PC/PG) or pH 7 buffer and TFE (50/50 buffer/TFE). TFE is known to promote helical structure and is used as a control. In buffer all peptides exhibited CD signatures consistent with random coil structure (minima ~198 nm). When bound to lipid vesicles, all of the full length peptides displayed CD spectral consistent with the formation of α-helical secondary structure (minima 208 and 222 nm) (Figure 10). Interestingly APX-17 showed less helical character than the shorter APX-12 which was clearly adopting helical structure. As anticipated, all peptides were shown to adopt a helical confirmation when in the presence of TFE.

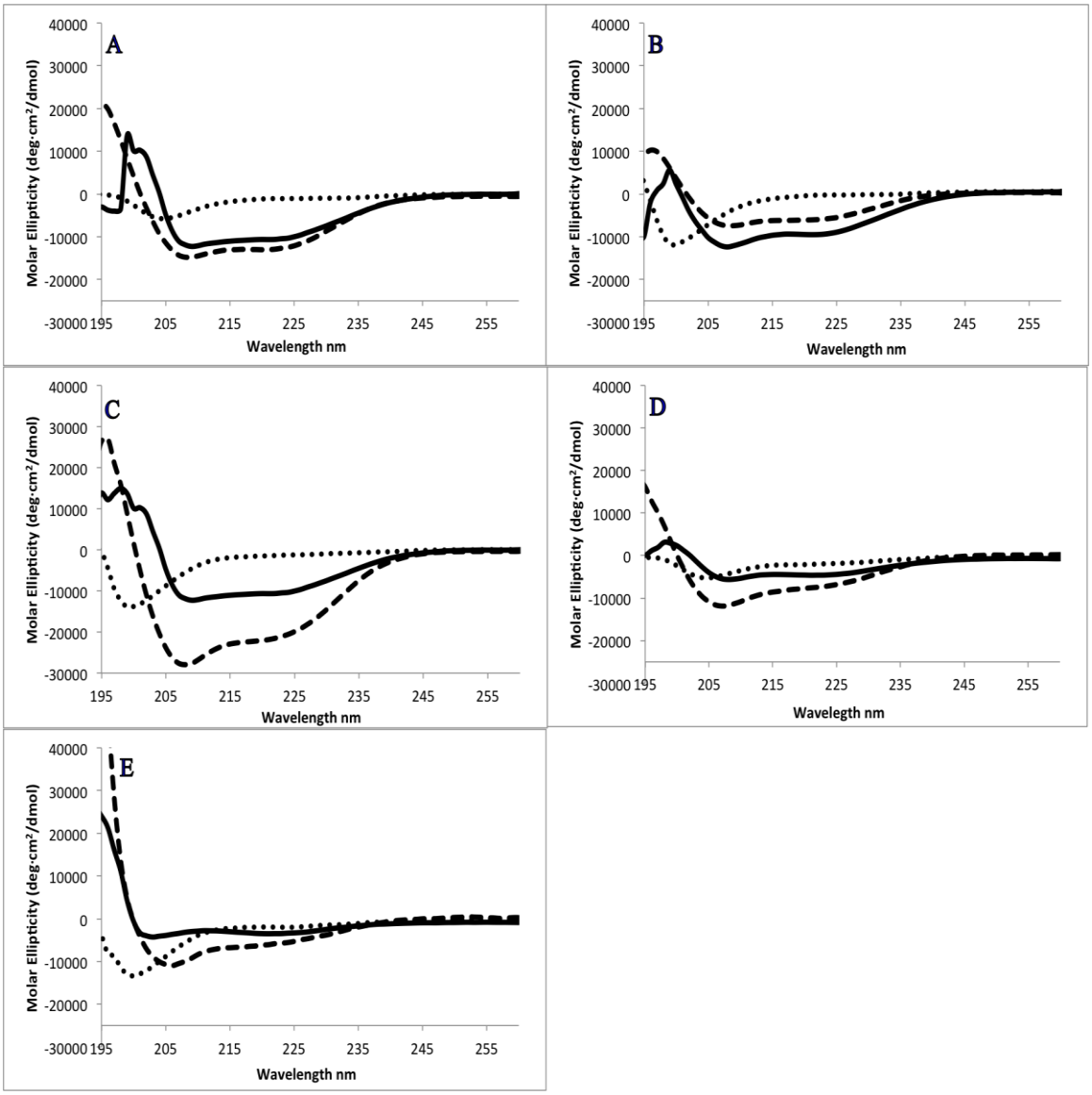

Figure 10. Circular Dichroism. Circular dichroism spectra of 5 μM (A) AP3, (B) AP3K, (C) APX, (D) APX-17, or (E) APX-12 Spectra were recorded in the presence of pH7 buffer, 1:1 TFE:pH7 buffer, or 250 μM 75:25 PC:PG SUVs. All spectra are averages of 64 scans and were background subtracted. For all graphs, buffer is shown as dots, TFE as dashes, and Lipid as solid line.

Calcein leakage. Bilayer disruption and or pore formation is commonly proposed to be a component of the mechanism of action of antimicrobial peptides. Calcein leakage assays were performed to determine if AP3 and analogs are capable of causing bilayer disruption allowing molecules to cross the membrane[64],[65]. In this assay, the fluorophore calcein is entrapped within lipid vesicles where fluorescence emission is strongly quenched through a self-quenching mechanism. If peptides induce bilayer disruption or create sufficiently large pores in the bilayer, the entrapped calcein can leak out of the vesicle lumen thus relieving the self-quenching and resulting in an increased in calcein fluorescence emission intensity. Leakage assays were performed using 75%/25% PC/PG vesicles and leakage was monitored over the course of 30 minutes, however the samples reached steady state after no more than 5 minutes in all cases. Full release was determined by adding an aliquot of the detergent Triton X-100 to each well after the 30 minute time course. The full-length peptides exhibit similar dose dependent vesicle permeabilization activity with near complete permeabilization achieved between 0.1-1 μM peptide. (Figure 11 and 12). Notably the truncated peptides induced minimal if any leakage even at the highest concentrations tested.

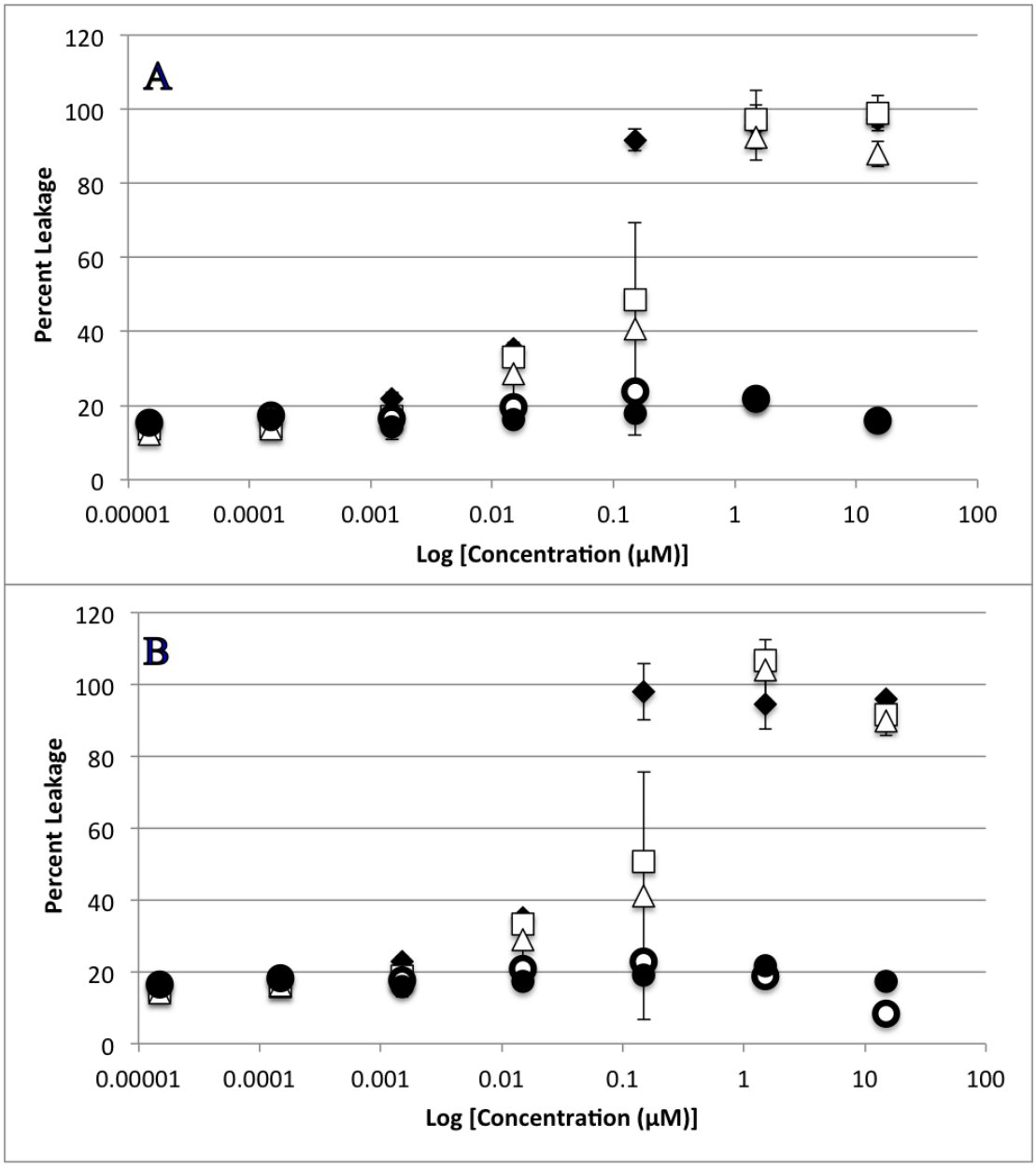

Figure 11. Vesicle Leakage Assay. Leakage of calcein entrapped in 75:25 PC:PG lipid vesicles after exposure to peptides. Percent leakage was calculated at 5 (A) and 30(B) minutes post addition of peptide. For both graphs, AP3 is shown as diamonds (◆), AP3K as squares (□), APX as triangle (Δ), APX-17 as open circle (❍), and APX-12 as closed circles (●). Lipid concentration in the sample was 200 μM Percent leakage was calculated by treating each sample with Triton X-100 and remeasuring fluorescence which was then set to 100% leakage. Each point represents the average of at least 3 replicate samples.

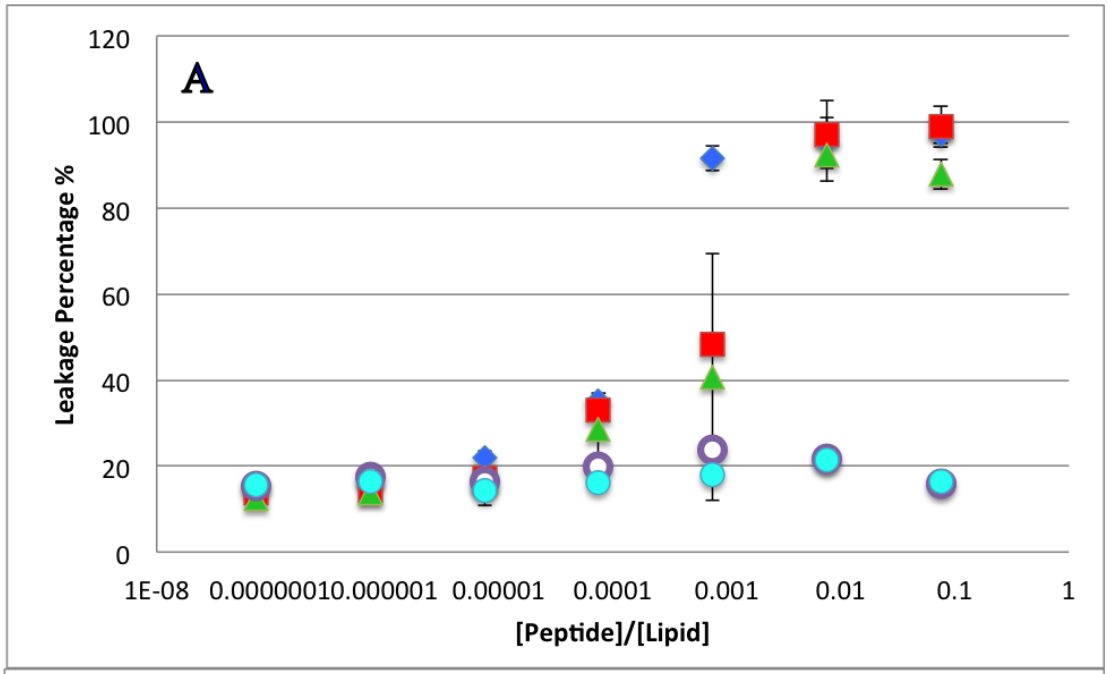

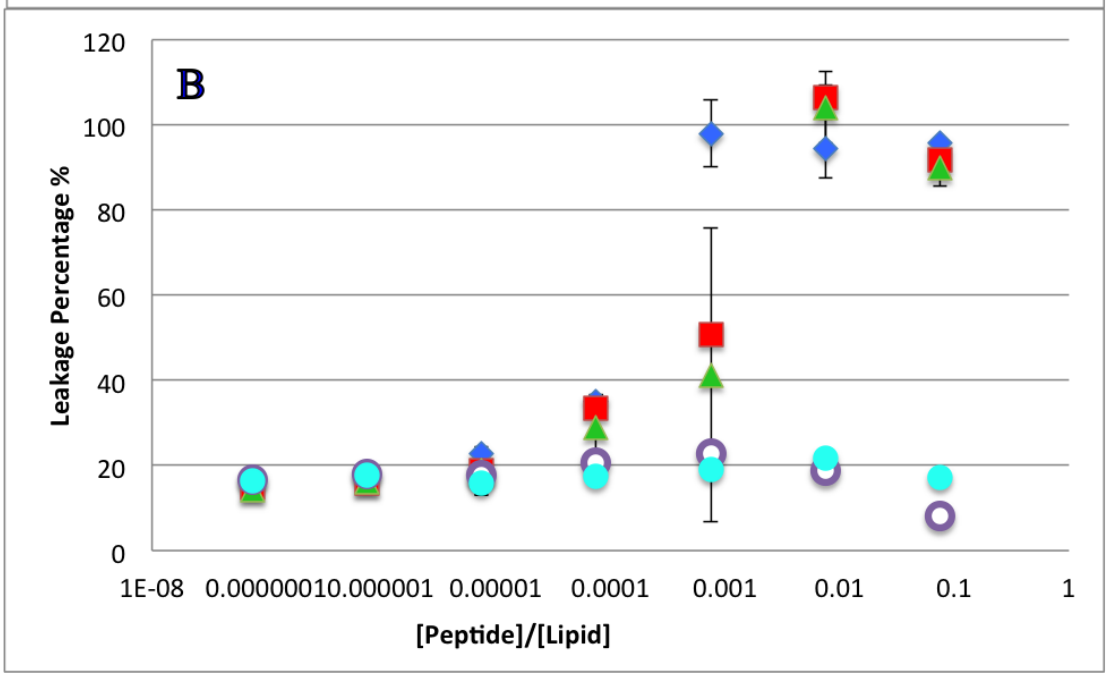

Figure 12. Calcein Leakage as a Function of Peptide/Lipid Concentration. Leakage of calcein entrapped in 75:25 PC:PG lipid vesicles after exposure to peptides. Percent leakage, as a function of peptide/lipid concentration, was calculated at 5 (A) and 30(B) minutes post addition of peptide. For both graphs AP3 is shown as diamonds (◆), AP3K as squares (■), APX as triangle (▲), APX-17 as open circle (❍), and APX-12 as closed circles (●). Lipid concentration in the sample was 200 μM Percent leakage was calculated by treating each sample with Triton X-100 and remeasuring fluorescence which was then set to 100% leakage. Each point represents the average of at least 3 replicate samples.

Bacterial membrane permeabilization. Based on the results of the calcein leakage assays, permeabilization of live, intact *E. coli* was investigated using enzyme based leakage assays. Briefly these assay rely on limited diffusion of a chromogenic substrate across a bacterial membrane(s). If the membrane(s) are disrupted by an antimicrobial peptide (or other agent) the substrate can more easily transit across the membrane(s) where it can be broken down by a bacterially expressed enzyme. The assay for outer membrane permeabilization relies on the enzyme β-lactamase, located in the *E. coli* periplasmic space, which can cleave the β-lactam containing molecule nitrocefin. The nitrocefin break down results in a chromogenic product[57],[66]. Bacteria were exposed to varying concentrations of the AP peptides and nitrocefin cleavage was monitored over a 90 minute time course. Figure 14 represents the data collected after 30 minutes of the assay (this was after samples had reached steady state) (Figure 13). The parent peptide AP3 exhibited the highest degree of bacterial membrane disruption followed closely by the other full-length peptides. Consistent with the calcein leakage data, the truncated peptides showed little to no disruption at any of the concentrations tested.

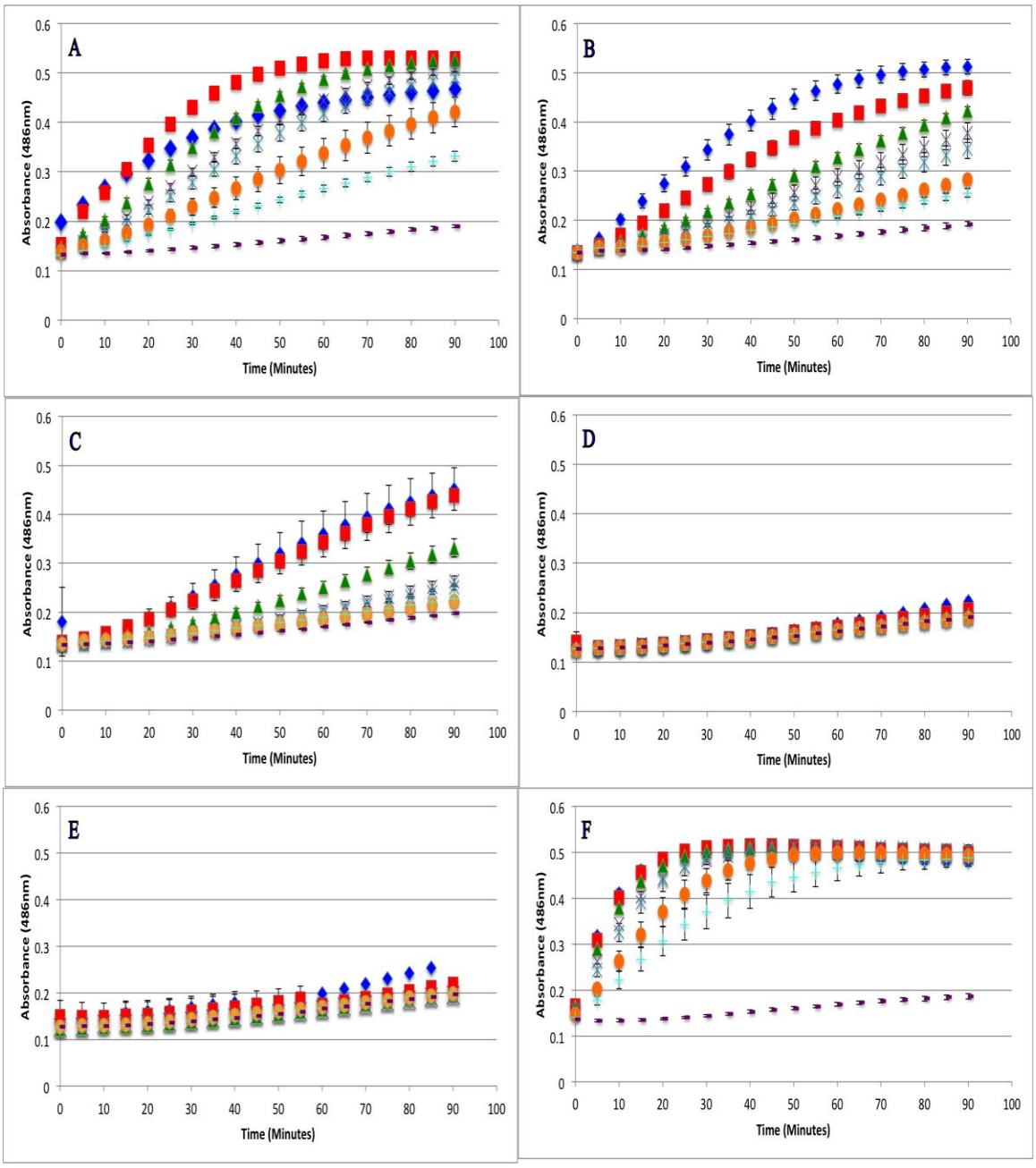

Figure 13. Outer-Membrane Permeability-Full Time Course. Outer-membrane permeability of *E. coli* after treatment with peptides (A) AP3, (B) AP3K, (C) APX, (D) APX-17, (E) APX-12 or (F) the control (Polymixin B). For all graphs peptide concentration 15 μM is shown as diamonds (◆), 7.50 μM as squares (■), 3.75 μM as triangle (▲), 1.88 μM as (X), 0.94 μM as (*), 0.47 μM as closed circles (❍), 0.23 μM as (+) and 0 μM as (-). Samples contained 50μg/mL nitrocefin, and 80μL of resuspended *E coli* cell suspension, and 10 μL peptide from a stock solution for the appropriate final concentration. Absorbance values shown represent data collected over 90 minutes of exposure to peptide. Data are averages of at least three replicate samples.

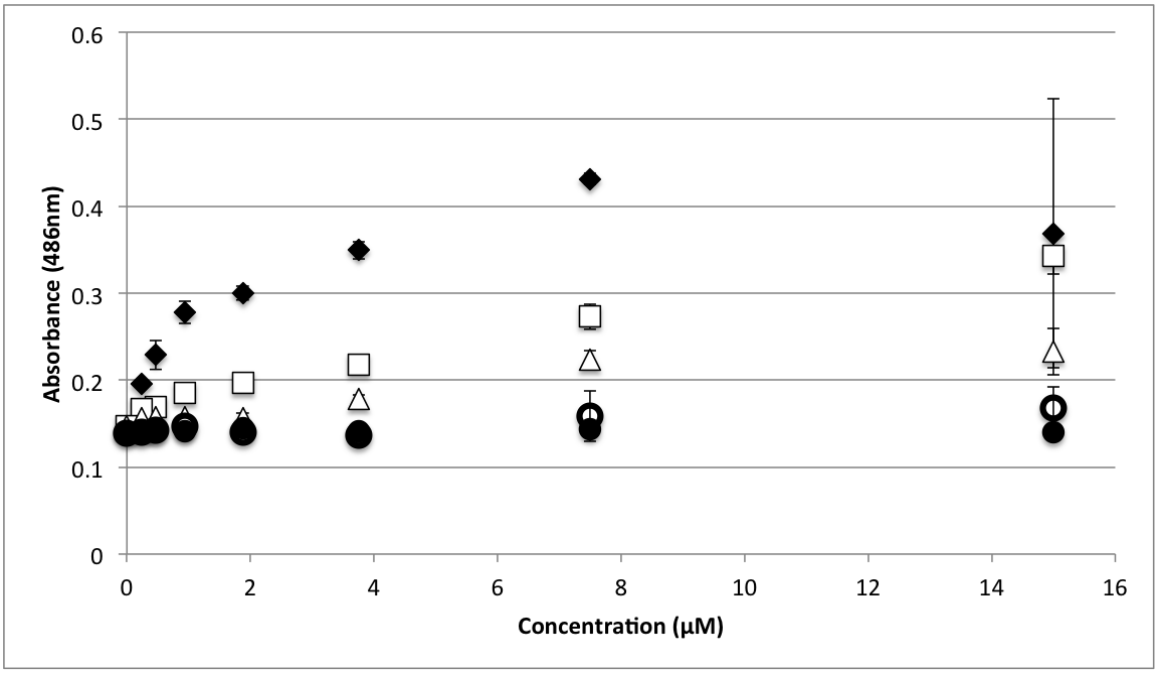

Figure 14. Outer-Membrane Permeability. Outer-membrane permeability of *E. coli* after treatment with peptides. For both graphs AP3 is shown as diamonds (◆), AP3K as squares (■), APX as triangle (▲), APX-17 as open circle (❍), and APX-12 as closed circles (●). Samples contained 50 µg/mL nitrocefin, and 80 µL of resuspended *E coli* cell suspension, and 10 µL peptide from a stock solution for the appropriate final concentration. Absorbance values shown represent data collected after 30 minutes of exposure to peptide. Data are averages of at least three replicate samples.

The assay for inner membrane permeabilization relies on the enzyme β-galactosidase, located in the *E. coli* inner membrane, which can cleave the molecule ONPG a chromogenic mimic of the natural substrate lactose. Similarly the ONPG cleavage results in a chromogenic product[57],[66]. Bacteria were exposed to varying concentrations of the AP peptides and ONPG break down was monitored over a 90 minute time course. Figure 16 represents the data collected after 30 minutes of the assay (this was after samples had reached steady state, Figure 15). Consistent with the results of the outer membrane permeabilization experiments, the parent peptide AP3 exhibited the highest degree of bacterial membrane disruption followed closely by the other full length peptides and little to no disruption induced by the truncated peptides.

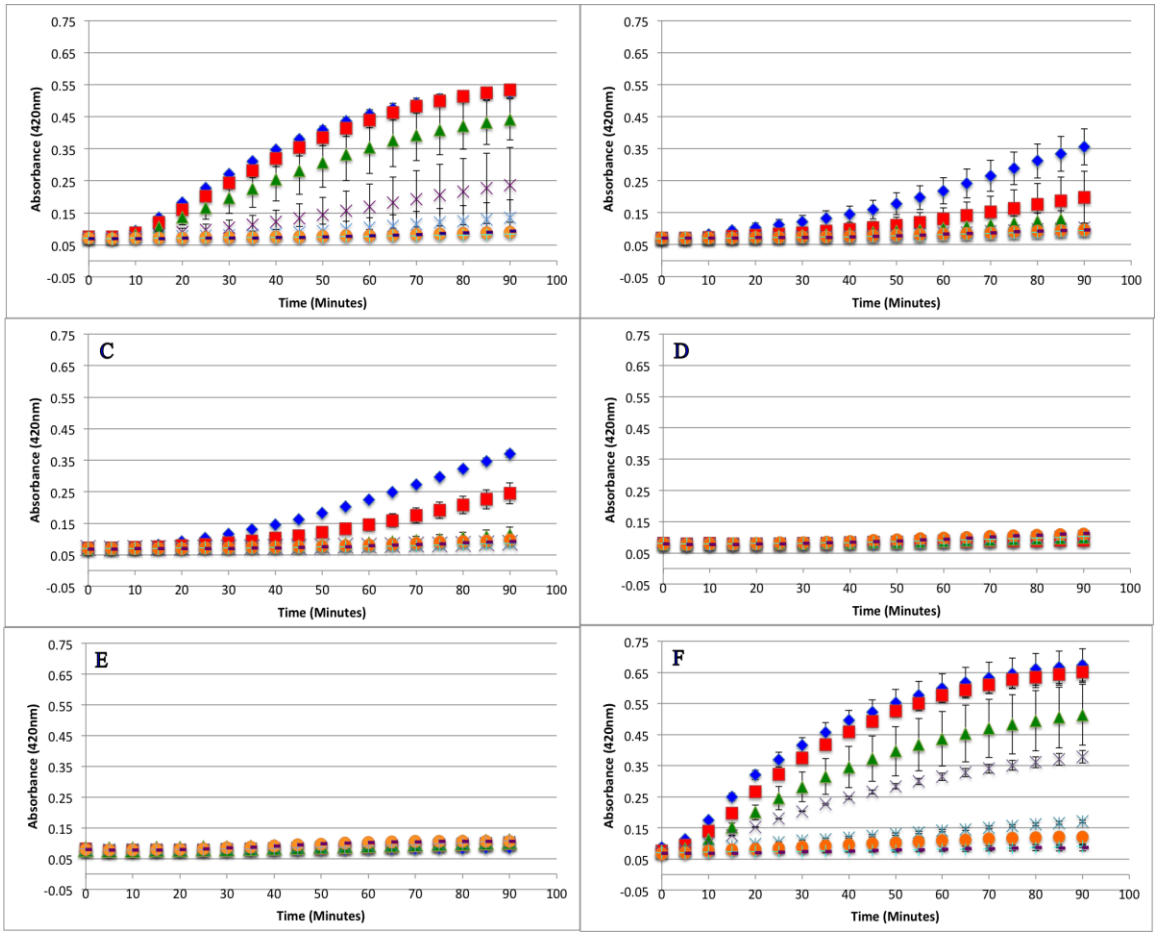

Figure 15. Inner-Membrane Permeability-Full Time Course. Inner-membrane permeability of *E. coli* after treatment with peptides (A) AP3, (B) AP3K, (C) APX, (D) APX-17, (E) APX-12 or (F) the control(C-Tab). For all graphs peptide concentration 15 µM is shown as diamonds (◆), 7.50 µM as squares (■), 3.75 µM as triangle (▲), 1.88 µM as (X), 0.94 µM as (*), 0.47 µM as closed circles (❍), 0.23 µM as (+) and 0 µM as (-). Samples contained 56.25µL Z-buffer (100 mM Na_2HPO_4, 10 mM KCl, 1 mM $MgSO_4$, 40 mM β– mercaptoethanol, pH 7.1), 12µL ONPG (4mg/ml), 18.75µL *E. coli*, (5.0×10^5 cfu/ml) and 10µL of peptide from the appropriate final concentrations. Absorbance values shown represents data collected after 90 minutes of exposure of peptide. Data are averages of at least three replicate samples.

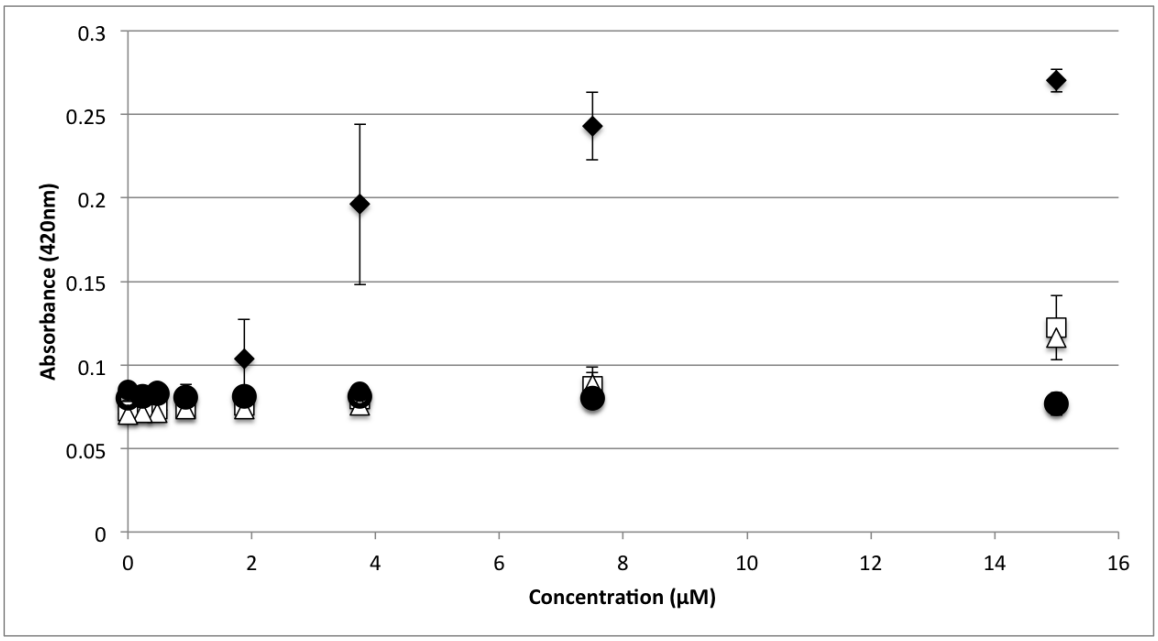

Figure 16. Inner-Membrane Permeability. Inner-membrane permeability of *E. coli* after treatment with peptides. For both graphs AP3 is shown as diamonds (◆), AP3K as squares (■), APX as triangle (▲), APX-17 as open circle (❍), and APX-12 as closed circles (●). Samples contained 56.25μL Z-buffer (100 mM Na_2HPO_4, 10 mM KCl, 1 mM $MgSO_4$, 40 mM β– mercaptoethanol, pH 7.1), 12μL ONPG (4mg/ml), 18.75μL *E. coli*, (5.0 x 10^5 cfu/ml) and 10μL of peptide from the appropriate final concentrations. Absorbance values shown represents data collected after 30 minutes of exposure of peptide. Data are averages of at least three replicate samples.

Mammalian cell viability. An MTT assay was performed to determine if the peptides exhibited any toxicity toward mammalian cells, in this case HEK-293 cells. The cells were treated with five different concentrations of each peptide ranging from 0.0015 μM to 15 μM. The results show that the peptides did not have any major inhibitory effect on the growth or viability of HEK-293 cells at the effective MIC concentrations (approximately 80 percent viable cells for AP3 and AP3K) (Figure 17)[67],[68],[69].

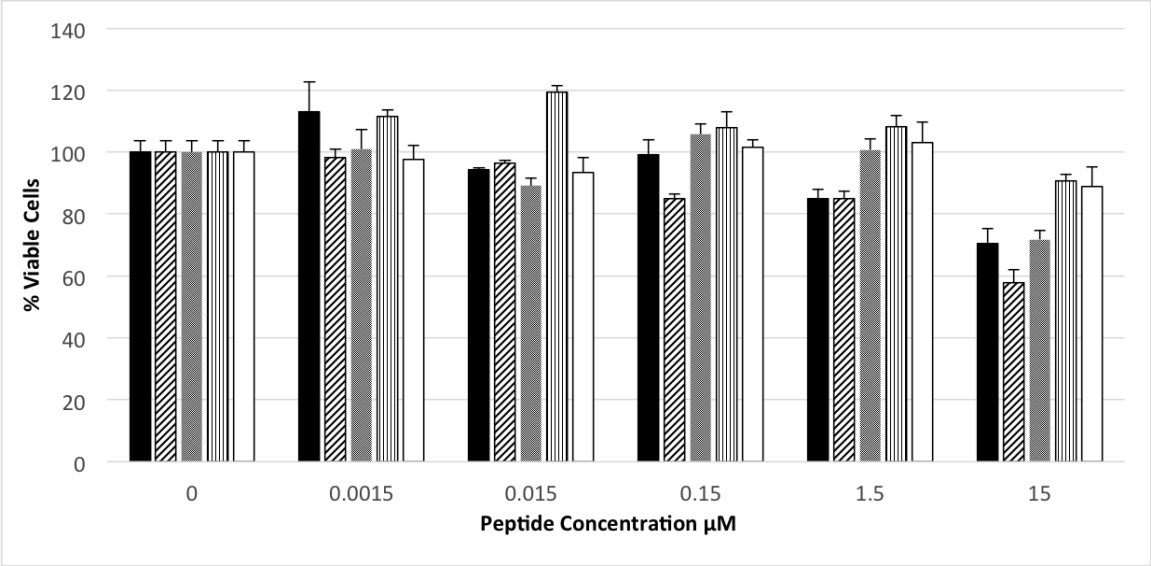

Figure 17. MTT Assay. Viability of human embryonic kidney HEK293 cells ($1.5x10^4$) measured with MTT assay after treatment of peptides and 24 h incubation. Peptides are represented as AP3 (black), AP3K (diagonal line), APX (gray), APX-17 (vertical lines) and APX-12 (white). Data are averages of at least three replicate samples.

Discussion

Antimicrobial resistance has become a global problem and the need for a solution by minimizing the amount of resistant bacteria has become crucial[4]. Finding alternatives to the use of antibiotics is a strategy that has been used to try and minimize the problem of resistance. Antimicrobial peptides are one class of molecules that have been investigated due to their low propensity for resistance along with their ability to kill or inhibit bacterial growth[26, 35]. We attempted to use this strategy to further explore a relatively unknown antimicrobial peptide along with various analogs. In an attempt to further enhance the efficacy of the peptides, a second antimicrobial agent, silver, was added to determine whether a synergistic relationship exists.

The data indicated all the peptides in this study interacted with lipid bilayers with similar affinities. This is interesting because, unlike many cationic AMPs, the inclusion of anionic lipids (POPG in our study) did not have a significant effect on lipid binding. Numerous reports indicate the increase in anionic lipid concentration increases the affinity for peptides for lipid bilayers[70],[71],[72]. The binding enhancement cause by inclusion of anionic lipid in a bilayer is driven by electrostatic interactions between cationic AMP and the anionic lipid surface, which mimics the bacterial cell surface[32]. Our results show even the truncated peptides, with decreased net positive charge, effectively bound to lipid bilayers over similar concentration ranges to the full length analogs (Figure 6), which is similar to behavior of LL-II and MSI-78 peptides[73],[74]. Additionally, penetratin and its truncates showed preferential binding to POPC/POPG membranes over DMPC/DMPG bilayers indicating a bilayer thickness effect[75]. The ability for peptides to span the bilayer is thought to be a component, or at least related to, the ability to disrupt lipid bilayer integrity and thus a link to hydrophobic matching is not unexpected[35],[71],[76].

Circular dichroism results indicate a clear formation of α-helical secondary structure for all AP3 peptides examined when they were bound to model lipid bilayers. This is consistent with numerous reports in the literature, indicating a random coil to helical confirmation change for cationic AMPs upon binding to lipid bilayers[57],[77]. Interestingly, the truncated peptides also adopted an α-helical confirmation when bound to a lipid bilayer, although to a lesser extent as evidenced by the lower mean residue ellipticity values[74]. This indicates the loss of hydrophobic and cationic groups does not

completely interfere with the ability of these peptides to adopt α-helical secondary structure[74].

For most antimicrobial peptides there is a clear facially amphiphilic structure when the peptide adopts an α-helical confirmation. Generally, cationic residues segregate to one face of the helix and hydrophobic moieties segregate to the opposite face[78, 79],[80]. However there is very little description in the literature of peptides that exhibit antimicrobial activity but do not adopt facially amphiphilic structures. Many reports focus on the facially amphiphillic structure as a necessary component of antimicrobial activity in peptides and polymers, often using non-facially amphiphillic controls which exhibit decreased efficacy. As seen in Figure 4, the AP3 and derivative peptides do not show any facial amphiphilicity, which could be tied to the insensitivity to anionic lipid composition. As the peptides are truncated, they lose both hydrophobic and cationic residues but this loss does not significantly effect the overall distribution of groups around the peptide helical axis. As such, it appears the hydrophobic burial interactions drive the binding of these peptides to the bilayer.

The binding to lipid membranes and helix formation in the AP3 peptides indicates they are behaving somewhat similar to traditional amphiphilic AMPs. However the lack of facial amphiphilicity presents an interesting question regarding how these peptides orient on/in the lipid bilayer. The lack of facial amphiphilicity makes traditional hydrophobic residue partitioning into the lipid bilayer difficult without also resulting in some burial of some hydrophilic groups. Acrylamide, an aqueous quencher of tryptophan fluorescence, was used to assay the orientation and topology of the AP3 peptides when bound to lipid bilayers. Strikingly the full-length peptides exhibited significantly different

quenching patterns compared to the truncated peptides. This indicates while all the peptides sequences studied bind to lipid bilayers, the final conformation at the bilayer surface is clearly different. Notably, the APX peptide series have the Trp at position 2 while the AP3 and AP3K have the Trp reporter at position 22, meaning in either a transmembrane or surface orientation, the Trp residue should be somewhat exposed to the aqueous milieu. The observed differences could be attributed to altering the charge/hydrophobic balance or as a result of hydrophobic mismatch between the shorter peptides and the bilayer.

Bacterial membrane permeabilization and vesicle leakage assays yielded consistent results in that full-length peptides caused a greater extent of leakage across the bilayer(s) compared to the truncated peptides. These results indicate that if the length and charge of an antimicrobial peptide is altered this can significantly lower the antimicrobial effectiveness, and potentially the mechanism of action, may be affected as reported elsewhere[81],[82, 83]. Depending on the mechanism of the shorten length of the truncated peptides may impact the ability to disrupt bilayers due to effects arising form hydrophobic mismatch[83],[84].

The MIC assay performed indicated the truncated peptides are less effective as antimicrobial agents compared to the full-length sequence, which is consist with recent reports in literature[85],[86],[87]. However, antimicrobial activity for AMPs is not exclusively linked to peptide length, as many naturally occurring AMPs are as short as the shortest sequences tested here[88],[89]. Similarly, reports in the literature have found that by decreasing the overall net charge of cationic AMPs the efficacy is also frequently

reduced[81]. The lack of antimicrobial activity for the truncated peptides in this study is not surprising considering the inability to permeabilize bacterial membranes.

The AP3 derived peptides also showed little cytotoxic activity at effective antimicrobial concentrations. This is consistent with the membrane permeabilization activity. Many studies have linked the cytotoxic effects of AMPs and AMP mimetics to hydrophobic interactions in which increased hydrophobic content is proportional to increased cytotoxicity.

The AP3 and APX peptide comparison is of interest as the only difference between these two peptides is the location of the Trp, yet there was a 4 fold difference in *S. aureus* MIC values and at least a two fold difference in *E. coli* MIC values. They seem to bind and quench similarly but have different permeabilization, This is surprising considering the small differences in the quenching and binding. The behavior in the leakage assay seems to mimic the behavior in the MIC assay more closely than the binding or the quenching assays. This reinforces the value of extending biophysical studies as well as natural membrane studies to better recapitulate the environment the peptides would encounter.

Conclusions

From the combination of the results (summarized in Table 6 and 7), the AP3 and derived peptides appear to bind to bilayers via hydrophobic interactions, but these hydrophobic interactions are not sufficient to cause significant cytotoxicity to mammalian cells or antibacterial activity in some cases. Additionally, binding to model lipid vesicles did not predict antimicrobial activity nearly as well as leakage assays. These results

highlight the delicate balance in structure activity relationships among antimicrobial peptides and warrant more in depth investigations.

Table 6

Overview of Results for AP Peptides

	Fluorescence Spectroscopy	**Circular Dichroism**	**MIC**	**MTT**
AP3	Large barycenter shift, indicating a change in tryptophan environment (small interaction with lipid vesicles). No binding preferences between 75:25 PC:PG and 100 PC lipid vesicles.	α helical confirmation in the presence of TFE and 75:25 lipid vesicles	Lowest MIC (high antimicrobial activity) against all organisms except *S. aureus*	Low toxicity at effective MIC values for HEK-293 cells
AP3K	No barycenter shift, indicating no change in tryptophan environment (small interaction with lipid vesicles). No binding preferences between 75:25 PC:PG and 100 PC lipid vesicles.	α helical confirmation in the presence of TFE and 75:25 lipid vesicles	Low MIC (high antimicrobial activity) against *S. aureus* and *P. aeruginosa*.	Low toxicity at effective MIC values for HEK-293 cells

Table 6 (continued)

	Fluorescence Spectroscopy	**Circular Dichroism**	**MIC**	**MTT**
APX	No barycenter shift, indicating no change in tryptophan environment (small interaction with lipid vesicles). No binding preferences between 75:25 PC:PG and 100 PC lipid vesicles.	α helical confirmation in the presence of TFE and 75:25 lipid vesicles	No measureable MIC value for *E. coli, K. pneumonia* and high MIC (low activity) for *S. aureus* and *P. aeruginosa*	Low toxicity for HEK-293 cells
APX-12	No barycenter shift, indicating no change in tryptophan environment (small interaction with lipid vesicles). No binding preferences between 75:25 PC:PG and 100 PC lipid vesicles.	α helical confirmation in the presence of TFE and 75:25 lipid vesicles	No measureable MIC value measured	Low toxicity for HEK-293 cells
APX-17	No barycenter shift, indicating no change in tryptophan environment (small interaction with lipid vesicles). No binding preferences between 75:25 PC:PG and 100 PC lipid vesicles.	α helical confirmation in the presence of TFE and 75:25 lipid vesicles	No measureable MIC value measured	Low toxicity for HEK-293 cells

Table 7

Overview of Leakage and Permeabilization Results for AP Peptides

	Calcein Leakage	**Outer Permeabilization**	**Inner. Permeabilization**
AP3	High (greatest of all peptide tested)	High (greatest of all peptides tested)	High (greatest of all peptides tested)
AP3K	High/moderate	Moderate/low	Moderate/low
APX	High/moderate	Moderate/low	Moderate/low
APX-12	Low/minimal	Low/little	Low/little
APX-17	Low/minimal	Low/little	Low/little

Chapter 3

Characterization, Antimicrobial Activity and Synergistic Effect of Decoralin and Silver Nitrate

Introduction

Venomous arthropods often produce venom mixtures that include peptides with antimicrobial activity. These complex venoms are naturally used to suppress prey[47]. The venom of the solitary eumenine wasp, *Oreumenes decoratus* is a mixture that includes an 11 residue peptide with is commonly referred to as decoralin[33]. Decoralin has been characterized as a linear, cationic alpha-helical peptide consisting of hydrophobic and basic amino acids[33]. Synthetic analogs of the original decoralin sequence have been characterized and the biological activities investigated[33]. In a study preformed by Konno et al., the C-terminus of decoralin was amidated, resulting in higher level of helicity and decreased hemolytic activity when compared to the original sequence[33]. The amidated analog of decoralin also showed greater antimicrobial activity against both Gram positive and Gram-negative bacteria[33]. These results show a great potential for decoralin analogs being a good template for new drug targets in combating antibiotic resistance.

In our current study, the original decoralin sequence has been modified to include a tryptophan residue in place of isoleucine. This analog was designed because tryptophan is a good reporter in fluorescence assays. The modified sequence of decoralin is shown in Table 8. This modified sequence was then tested in various assays including fluorescence spectroscopy, circular dichroism (CD) spectroscopy, vesicle permeabilization assays, bacterial permeabilization assays, and minimal inhibitory concentration (MIC) assays to further characterize this venom peptide.

Material and Methods

Bacterial culturing. Prepared using the procedure described in Chapter 2.

Minimum inhibitory assay (MIC). Same procedure performed as described in Chapter 2.

Lipid preparation. Prepared using the procedure as described in Chapter 2.

Binding experiments. Same procedure performed as described in Chapter 2.

Acrylamide quenching. Same procedure performed as described in Chapter 2.

Circular dichroism. Same procedure performed as described in Chapter 2.

Calcein leakage assay. Same procedure performed as described in Chapter 2.

Bacterial outer membrane permeabilization assay. Same procedure performed as described in Chapter 2.

Bacterial inner membrane permeabilization assay. Same procedure performed as described in Chapter 2.

Bacterial growth analysis. Dilutions were grown to OD_{600} 0.2 - 0.3 before being diluted a second time to a range calculated by the experiment being performed. Calculations were performed using the conversion factors of OD_{600} = 1.0 is equivalent to ~10^8 CFU/mL for *S. aureus* and *K. pneumoniae* and ~10^9 CFU/mL for *E.coli* and *P. aeruginosa*[90],[91],[92].

Synergy assay. Assays for synergistic interactions between peptides and Ag^+ were performed using the checkerboard microdilution method[93],[94]. Briefly, plates are set up similarly to the MIC assay, however combinations of antimicrobial peptides and $AgNO_3$ were added to the wells.

Results

Lipid binding. As described in Chapter 2, binding experiments were used to investigate the interaction between the peptide decoralin with model lipid bilayer. Since the modified decoralin sequence contains a tryptophan residue, tryptophan emission fluorescence spectroscopy was used to monitor the environmental changes of the peptide. Model vesicles were composed of either 100% PC or 75/25% PC/PG lipids to investigate the effect of electrostatics on the binding of peptides to bilayers. Our results showed that decoralin exhibited a shift in emission barycenter when bound to the 75%/25% POPC/POPG lipid composition (Figure 18 and 19). In contrast the peptide exhibited less shift in emission barycenter when titrated with 100% PC, vesicles indicating the peptide likely adopts a somewhat different orientation at the bilayer surface in these vesicles.

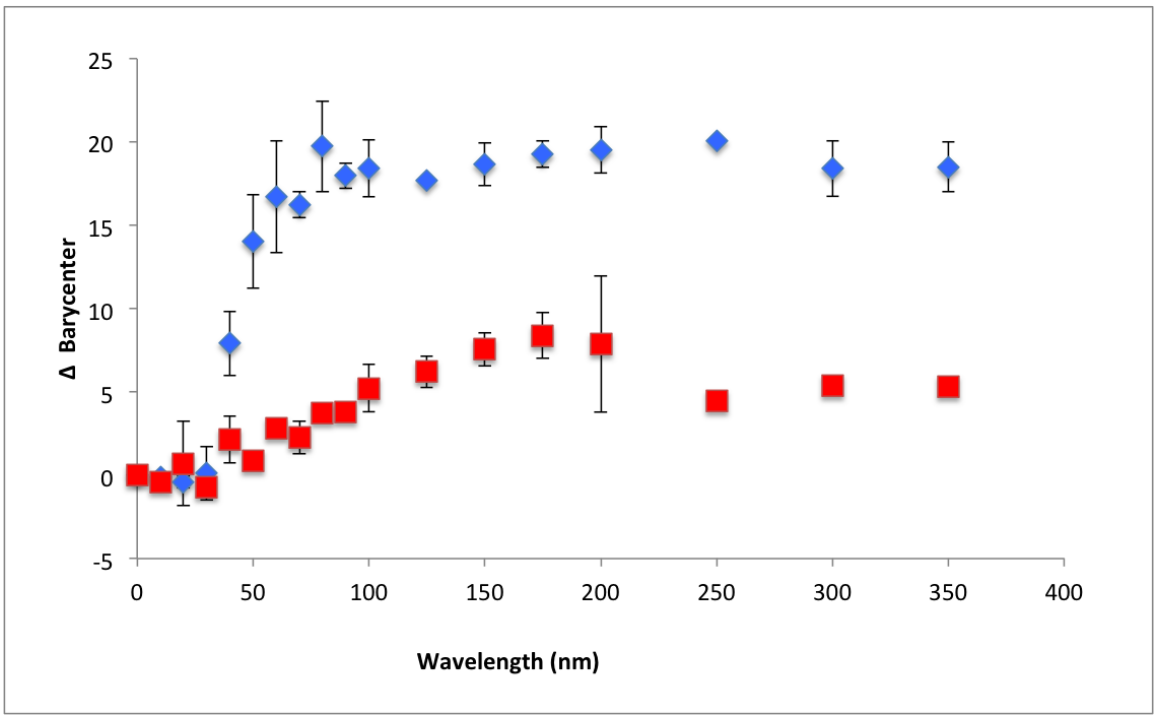

Figure18. Decoralin Binding to Lipid Vesicles by Spectral Shifts. Binding of decoralin to lipid vesicles analyzed by change in emission spectrum barycenter as a function of lipid concentration. Decoralin was titrated with either 75:25 PC:PG (◆) and 100 PC (■) vesicles. Peptide concentration was 2 μM both cases. Data shown are corrected for background fluorescence and represent averages of at least three replicate samples.

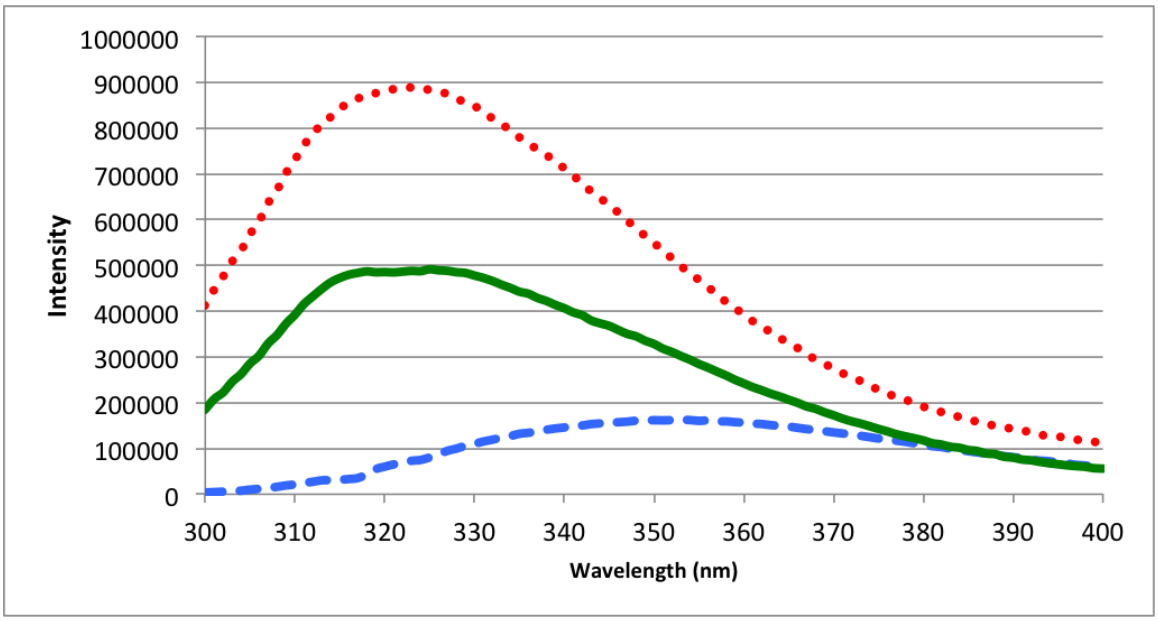

Figure 19. Barycenter Shift of Decoralin. Barycenter shift of decoralin at lipid vesicles at concentrations of 0, 90, and 300 μM. Lipid compositions titrated were 75:25 PC:PG. Data are averages of at least three replicate samples.

Fluorescence quenching. In an attempt to analyze the topography of decoralin on the bilayer surface, fluorescence quenching experiments were performed. The aqueous quencher acrylamide was chosen as it effectively quenches tryptophan and can readily pass across lipid bilayers. The results of quenching experiments in the absence and presence of PC/PG vesicles are shown. The results indicate there is little difference in quenching, thus the tryptophan appears to be very accessible to aqueous environments and therefore the acrylamide quencher, in both bound and unbound states (Figure 20).

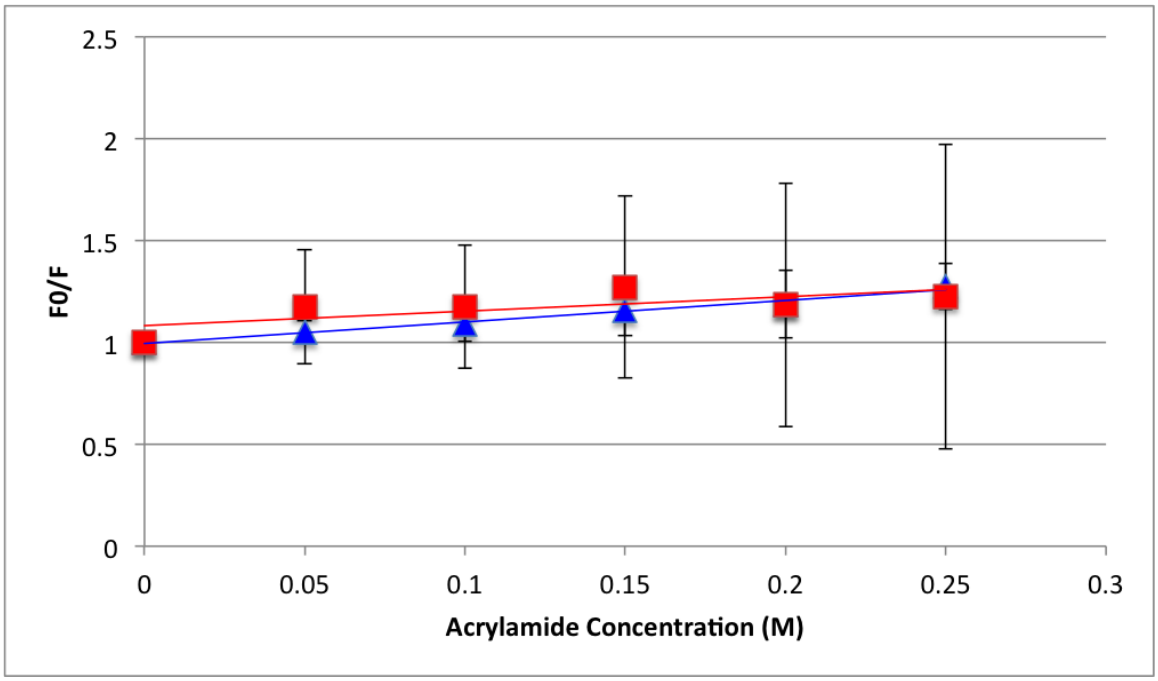

Figure 20. Fluorescence Quenching of Decoralin. Fluorescence quenching of decoralin by acrylamide in the presence (◆) or absence (■) of lipid vesicles. Quenching of 2 μM peptide at pH 7 is shown in the presence of 75:25 POPC:POPG vesicles and100 POPC vesicles both totaling a final concentration of 250 μM. Data shown are corrected for background fluorescence, inner filter effects, and are averages of at least three replicate samples.

Circular dichroism. CD spectra were collected for peptides dissolved in pH 7 buffer, pH 7 buffer with lipid vesicles (75/25% PC/PG) or pH 7 buffer and TFE (50/50 buffer/TFE). TFE is known to promote helical structures and is used as a comparison. In buffer, decoralin exhibited CD spectra consistent with a random coil structure (minimum at ~198 nm), in the presence of TFE exhibited decoralin exhibited CD spectral consistent with the formation of α-helical secondary structure (minima 208 and 222 nm) (Figure 21). In the presence of lipid vesicles, the peptide clearly adopts an α-helical

confirmation, consistent with the behavior of many known membrane disruptive peptides such as melittin and magainin.

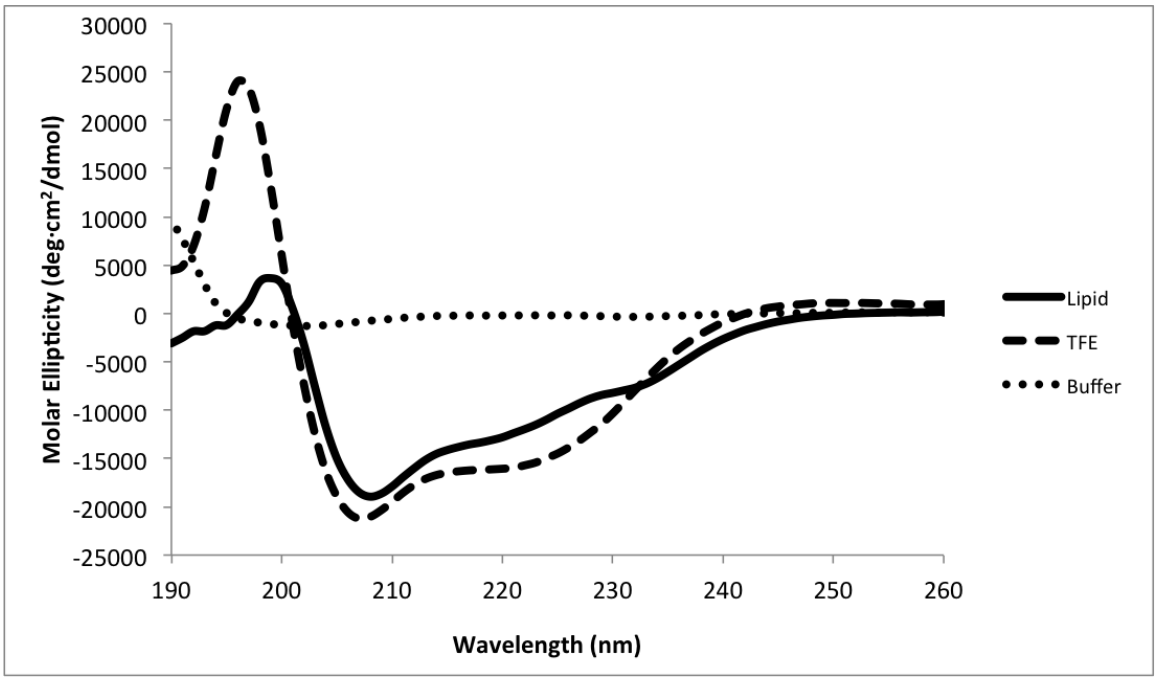

Figure 21. Circular Dichroism of Decoralin. Circular dichroism spectra of 5 μM decoralin. Spectra were recorded in the presence of pH7 buffer, 1:1 TFE:pH7 buffer, or 250 μM 75:25 PC:PG SUVs. All spectra are averages of 64 scans and were background subtracted. For all graphs, buffer is shown as dots, TFE as dashes, and Lipid as solid line.

Calcein leakage. Calcein leakage assays were performed on decoralin to determine the ability to disrupt model lipid vesicles (75%/25% PC/PG). At the highest peptide concentration tested, decoralin exhibited moderate bilayer disruption (~60 to 70 percent release) at both the 5 and 30 minutes time points (Figure 22). As seen with the AP peptides, steady-state was achieved shortly after the peptide was added resulting in a small between the 5 and 30 minute time points. Leakage was also determined for another insect-derived peptide, L1. This peptide is significant longer than the decoralin sequence and thus may have different interacting properties. This peptide exhibited slightly lower peptide induced leakage from vesicles.

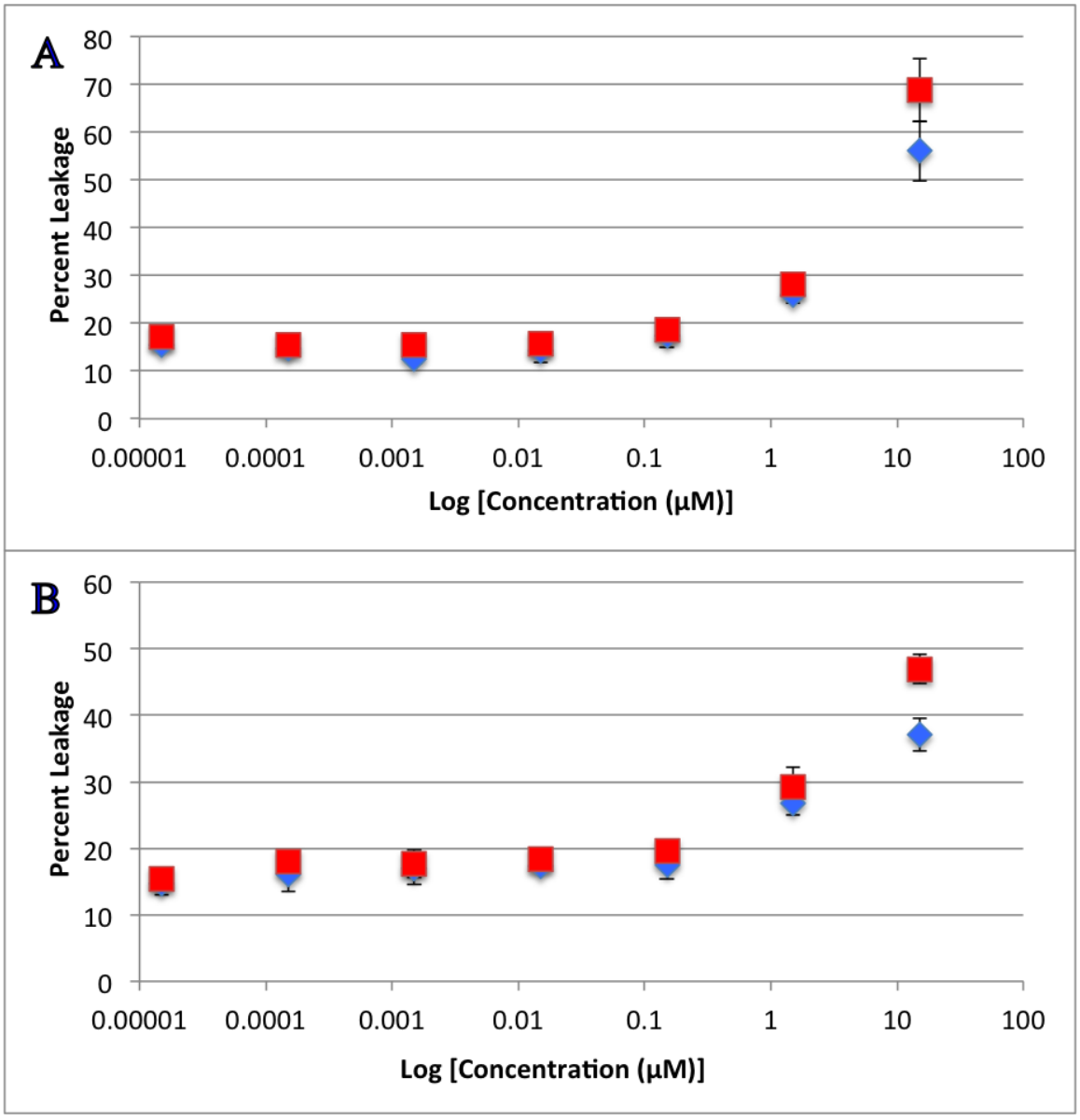

Figure 22. Vesicle Leakage Assay of Decoralin and L1. Leakage of calcein entrapped in 75:25 PC:PG lipid vesicles after exposure to peptides. Percent leakage of lipid after exposure of decoralin (A) and L1 (B). For both graphs, 5 minutes of leakage is shown as diamonds (◆), and 30 minutes of leakage as squares (■). Lipid concentration in the sample was 200 µM Percent leakage was calculated by treating each sample with Triton X-100 and remeasuring fluorescence which was then set to 100% leakage. Each point represents the average of at least 3 replicate samples.

Bacterial membrane permeabilization. As described previously, bacterial membrane permeabilization was used to further investigate the membrane disruption ability of peptide in question. These experiments provide a more authentic evaluation of whether a peptide can disrupt natural bacteria membranes. Consistent with calcein leakage assays, decoralin showed moderate amount of membranes disruption only at the highest concentrations tested (Figure 23 and 24). For both the outer and inner membrane permeabilization was time dependent with the continuing increase in chromophore conversion over the entire 90 minute time course study.

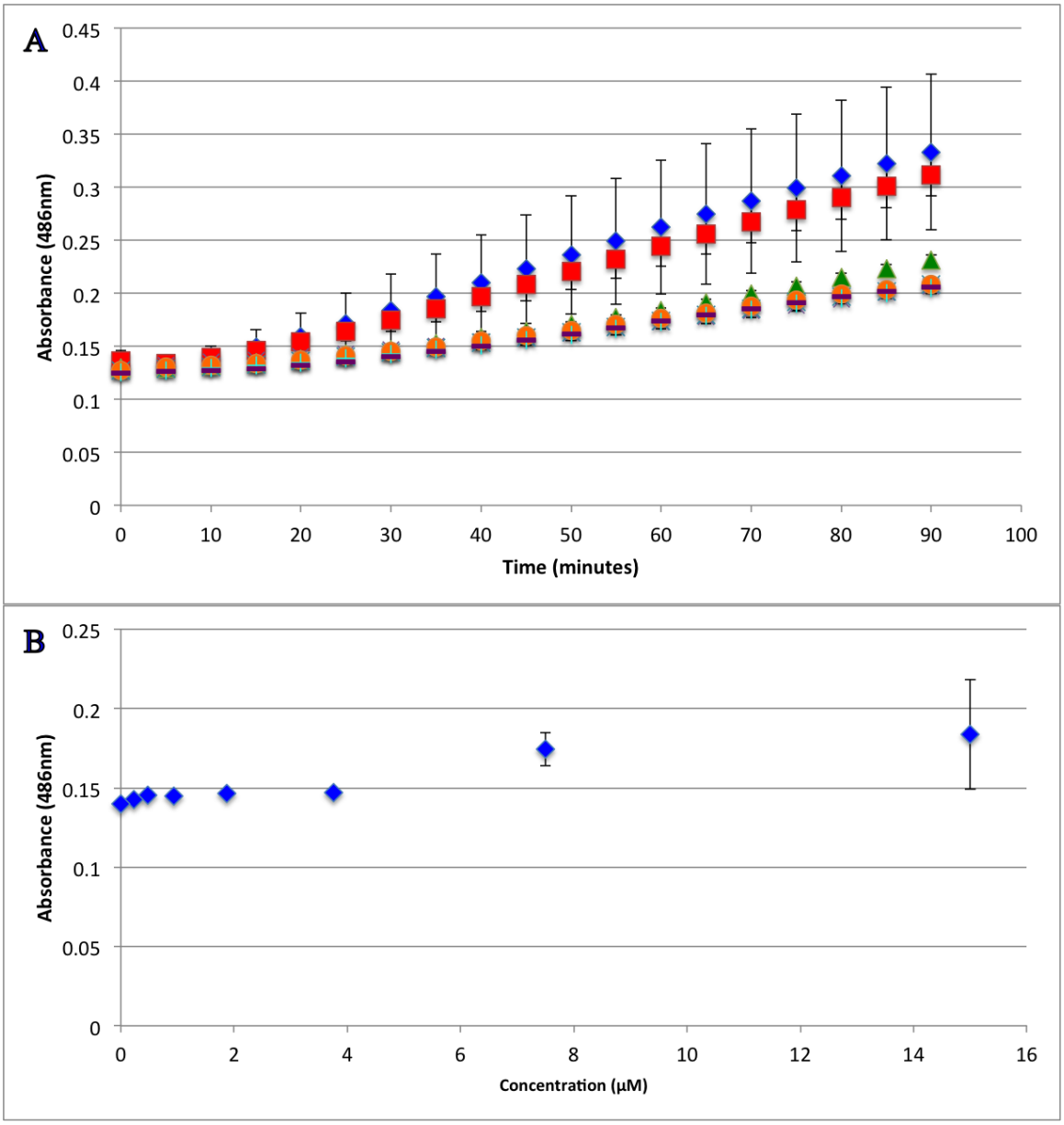

Figure 23. Outer-Membrane Permeability of *E. coli* With Decoralin. Absorbance values shown represent data collected over 90 minutes (A) and 30 minutes (B) of exposure to decoralin. For graph (A) peptide concentration 15 μM is shown as diamonds (◆), 7.50 μM as squares (■), 3.75 μM as triangle (▲), 1.88 μM as (X), 0.94 μM as (*), 0.47 μM as closed circles (❍), 0.23 μM as (+) and 0 μM as (-). Samples contained 50 μg/mL nitrocefin, and 80 μL of resuspended *E coli* cell suspension, and 10 μL peptide from a stock solution for the appropriate final concentration. Data are averages of at least three replicate samples.

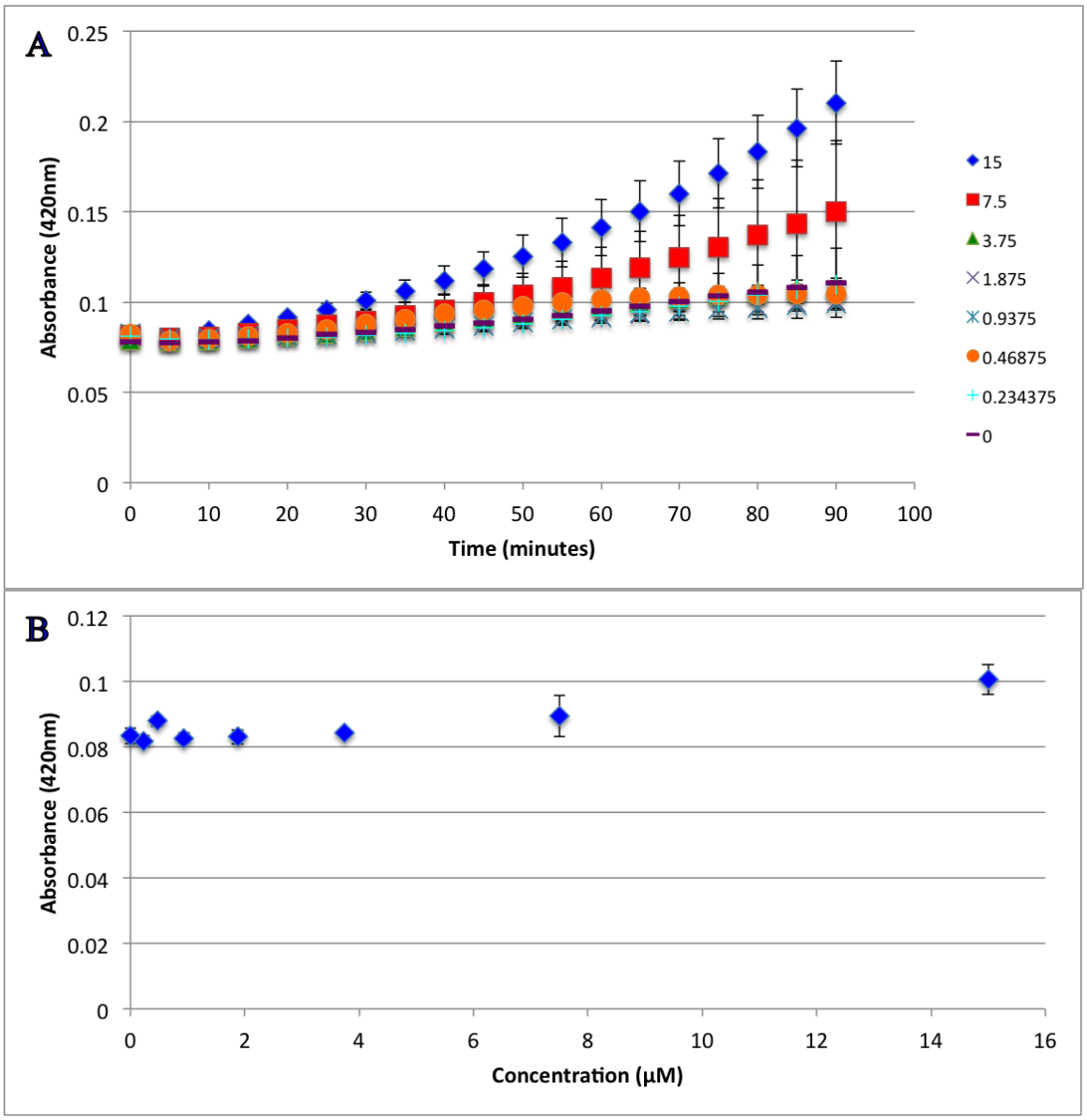

Figure 24. Inner-Membrane Permeability of *E. coli* With Decoralin. Absorbance values shown represent data collected over 90 minutes (A) and 30 minutes (B) of exposure to decoralin. For graph (A) peptide concentration 15 μM is shown as diamonds (◆), 7.50 μM as squares (■), 3.75 μM as triangle (▲), 1.88 μM as (X), 0.94 μM as (*), 0.47 μM as closed circles (❍), 0.23 μM as (+) and 0 μM as (-). Samples contained 56.25μL Z-buffer (100 mM Na_2HPO_4, 10 mM KCl, 1 mM $MgSO_4$, 40 mM β– mercaptoethanol, pH 7.1), 12 μL ONPG (4 mg/mL), 18.75 μL *E. coli*, (5.0 x 10^5 CFU/mL) and 10 μL of peptide from the appropriate final concentrations. Data are averages of at least three replicate samples.

Antibacterial activity. MIC assays were performed to determine the efficacy of decoralin against various Gram-negative and Gram-positive bacteria. Decoralin had the lowest MIC (highest activity) against *E. coli* exhibiting an MIC of approximately 5μM and a two-fold increase of 10 μM against *S. aureus*. The bacterial species *P. aeruginosa* and *K. pneumonia* were also tested but decorlain exhibited no antimicrobial activity against these species for the concentrations tested. MIC values were also determined for the L1 peptide, which exhibited the lowest MIC values for *E. coli* and *S. aureus* at approximately 1.81μM and 7.25μM respectively. In contrast L1 was active against *K. pneumonia* and *P. aeruginosa* exhibiting an MIC of 14.5μM in both cases. MIC assays were also performed using the small molecule silver nitrate, which exhibited activity against all species tested ranging from 12.5 to 50 μM (Table 8 and 9).

Combinatorial MIC were performed with peptides and silver nitrate to determine if antimicrobial synergy between these compounds exist. L1, and silver nitrate alone, combinatorial MIC assays were performed to see if an enhanced efficacy existed. The combination of both silver and peptides (decoralin or L1) lowered the MIC values for the bacteria species *E. coli* and *S. aureus* when compared to either peptide or silver nitrate alone(Table 8 and 9). In contrast, the MIC against *P. aeruginosa* and *K. pneumonia* remained unchanged or were only slightly affected by the presence of both antimicrobial species.

Table 8

Combinatorial MIC (μM) for S. aureus, E. coli, P. aeruginosa, and K. pneumonia with Decoralin

MIC (μM) for *S. aureus*, *E. coli*, *P. aeruginosa*, and *K. pneumoniae*				
	S. aureus	*E. coli*	*P. aeruginosa*	*K. pneumoniae*
Decoralin	10	5	>10	>10
Silver Nitrate	50	25	25	25
Silver Nitrate (w/Constant 2 **μM** Decoralin)	12.5	6.25	>10	6.25
Decoralin (w/ Constant 5 **μM** Silver Nitrate)	5	0.625	>10	>10

Table 9

Combinatorial MIC (μM) for S. aureus, E. coli, P. aeruginosa, and K. pneumonia with L1

MIC (μM) for *S. aureus*, *E. coli*, *P. aeruginosa*, and *K. pneumoniae*				
	S. aureus	*E. coli*	*P. aeruginosa*	*K. pneumoniae*
L1	7.25	1.8125	14.5	14.5
Silver Nitrate	50	12.5	25	12.5
Silver Nitrate (w/Constant 2 **μM** L1)	12.5	0.39	12.5	6.25
L1 (w/ Constant 5 **μM** Silver Nitrate)	5	1.25	14.5	14.5

Bacterial growth kinetics experiments were performed to observe the effects of the decoralin and silver nitrate in a liquid culture of bacteria. Kinetic experiments were performed over a three hour time period comparing bacterial growth in an untreated control to that in the presence of decoralin silver nitrate or both. The preliminary results show that the *S. aureus* was most affected by the combination of silver nitrate and decoralin compared to either treatment alone, indicating an additive or synergistic activity. In contrast, the *E. coli* culture exhibited no inhibition of growth under the conditions tested (Figure 25).

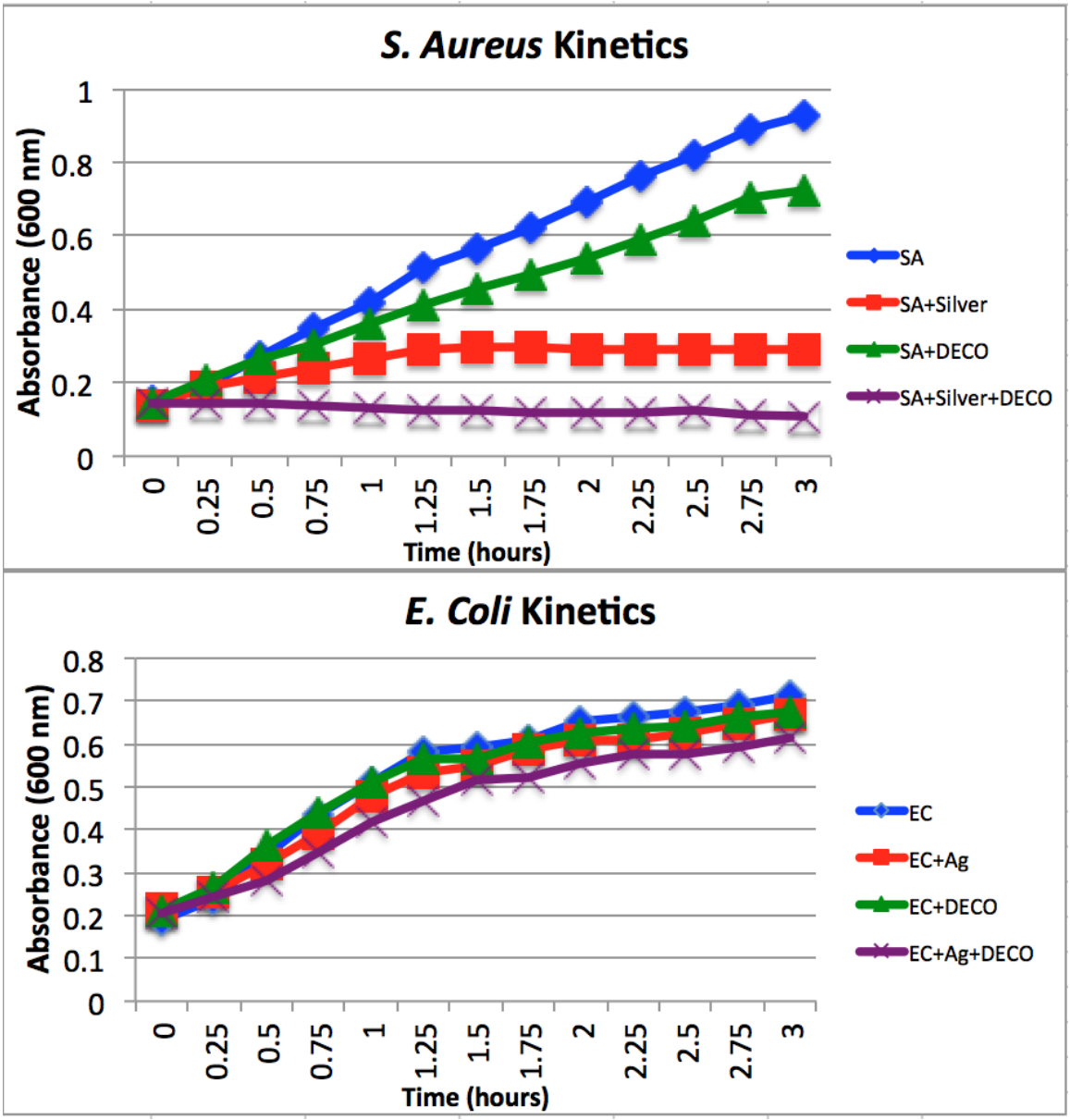

Figure 25. Kinetics of *E. coli* and *S. aureus* With Decoralin. Growth kinetics of *E. coli* and *S. aureus* after the addition of decoralin. Bacterial dilutions grown to OD_{600} 0.2 - 0.3 before being diluted a second time to a range calculated by the experiment being performed. Calculations were performed using the conversion factors of OD_{600} = 1.0 is equivalent to ~10^8 CFU/mL for *S. aureus* and ~10^9 CFU/mL for *E.coli*. Four samples were used; control (just bacterial) shown as diamonds (◆), bacteria combined with silver nitrate shown as squares (■), bacteria combined with decoralin shown as triangle (▲) and bacterial, silver nitrate and decoralin shown as (X). Kinetics experiments were performed over 3 hour time period with absorbance readings taken every 15 minutes.

Potential synergistic interactions were investigated using checkerboard assays[95-97]. Briefly these assays are set up to vary two different components added to a bacterial culture to evaluate effects of interactions. These assays were performed using varying concentration of both silver nitrate and peptide to determine whether the combination had an enhanced antimicrobial effect. The peptide decoralin was tested and the results showed no synergistic effect. This was also found to be the case for the L1 peptide against *E. coli*. Although no synergistic effect was observed, there appears to be some additive effects, consistent with results in Figure 26 and 27, with the MIC values being lower in the presence of both antimicrobial species.

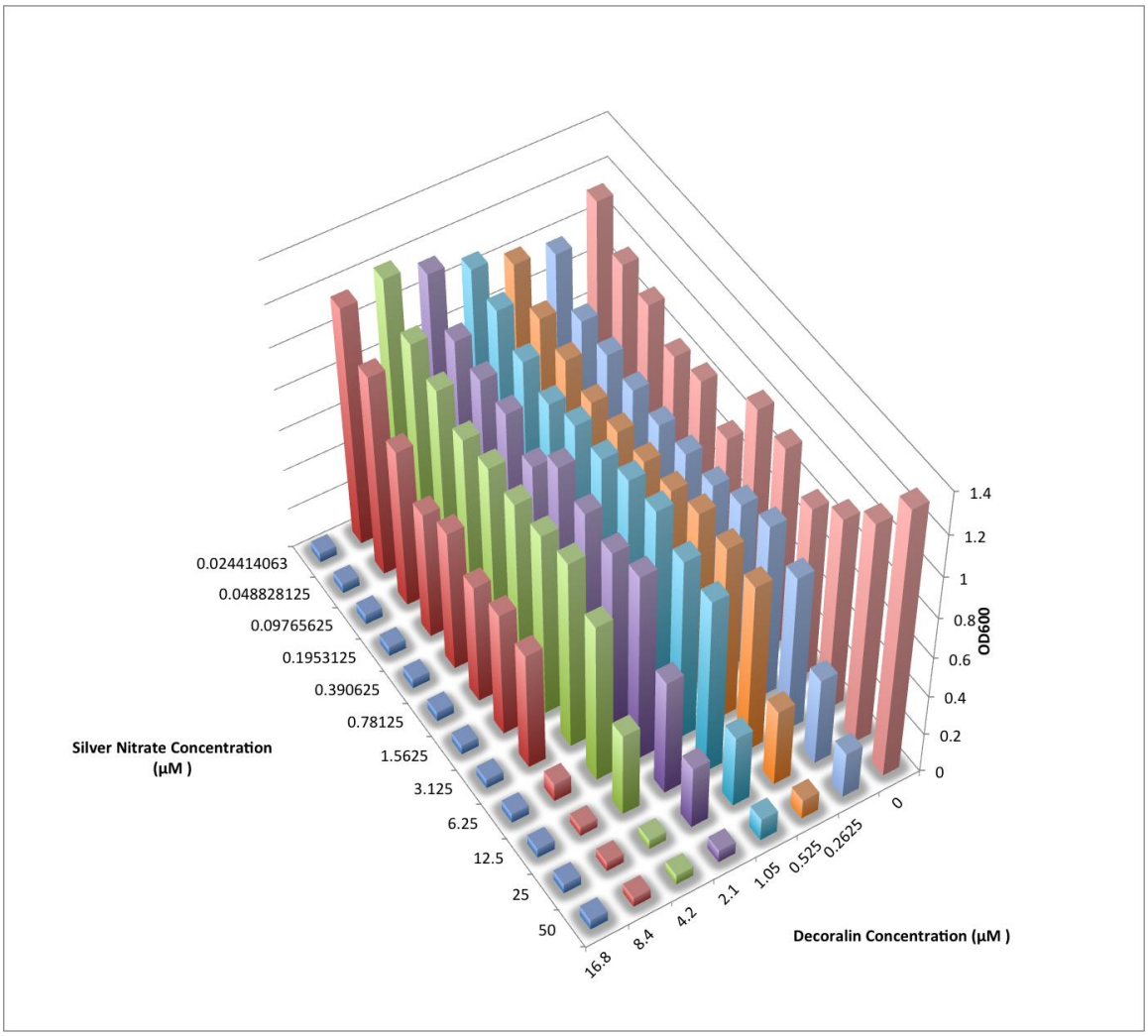

Figure 26. Synergy of Decoralin and Silver Nitrate. Synergistic assay of the peptide Decoralin with the addition Silver Nitrate. Assay was done using the bacteria species *S. Aureus*. Assay plate was made by adding 10 µL of the diluted peptide stock solutions, 10 µL of varying silver nitrate concentration and then 80 µL of diluted bacterial culture. The final bacterial load was ~5.0 x 10^5 cfu/mL as calculated from OD_{600} measurements of a log-phase culture. The assay plate was incubated at 37 $^{\circ}$C for 18 h. Bacterial growth was assayed by absorbance at OD_{600}.

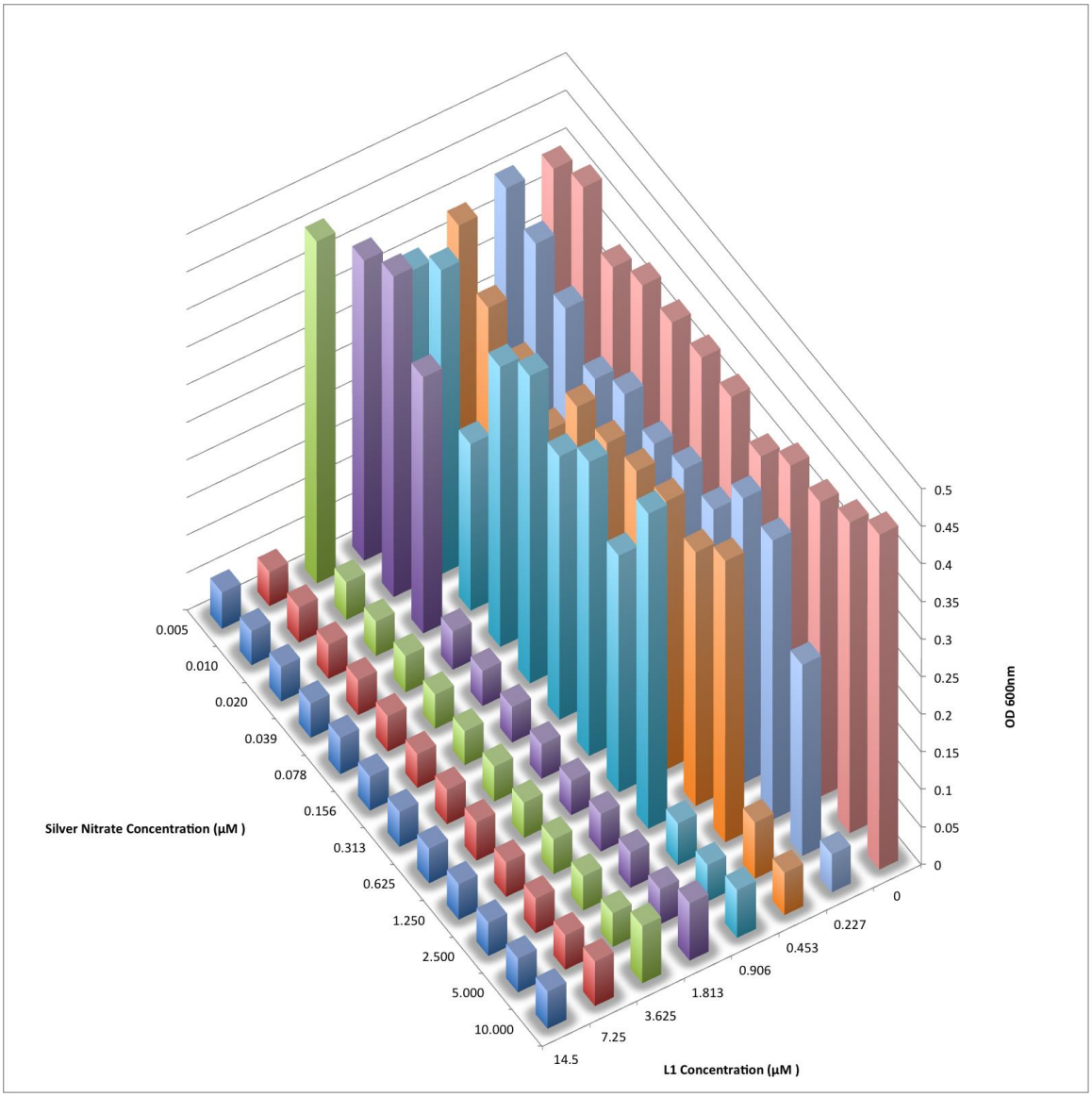

Figure 27. Synergy of L1 and Silver Nitrate. Synergistic assay of the peptide L1 with the addition Silver Nitrate. Assay was done using the bacteria species *E. Coli.* Assay plate was made by adding 10 µL of the diluted peptide stock solutions, 10 µL of varying silver nitrate concentration and then 80 µL of diluted bacterial culture. The final bacterial load was ~5.0 x 10^5 cfu/mL as calculated from OD_{600} measurements of a log-phase culture. The assay plate was incubated at 37 ˚C for 18 h. Bacterial growth was assayed by absorbance at OD_{600}.

Discussion

Antimicrobial peptides have been of great interest for development into therapeutics because of the broad spectrum of antimicrobial activity these molecules exhibit. There are also remaining questions over the mechanism of action of these peptides, especially considering the evolutionary diversity seen in nature. Additionally antimicrobial peptides are derived from multiple sources including host defense peptides and peptides from venom, which in turn may act through different mechanism based on their origin. As such, it's of great interest to compare peptides from these different classes. Specifically the relationship between sequence and mechanism of action may differ between the classes as well as potential to the peptide and the second is being the potential for these peptides to interact with each other and other antimicrobial agents to exert combinatorial effect.

The linear cationic peptide decoralin which was originally isolated from the venom of the solitary eumenine wasp *Oreumenes decoratus* was chosen to investigate as a comparison to the truncated AP peptides. Decoralin is a short peptide (11 amino acid residues) that exhibited antimicrobial activity against some of bacterial species tested. Decoralin is a short peptide therefore may act via a mechanism of action that is different when compared to longer peptides such as AP3. In addition, the truncated APX-12 and APX-17 exhibited lost antimicrobial activity when the amino acid sequence was shortened from the originals APX sequence. The contrast between the APX-12 peptide and decoralin presents an interesting question on sequence and mechanism of action. We wanted to investigate and compare the size and charges of each of these peptides to determine how these characteristics affected the antimicrobial activity. In addition, we

also investigated the slightly longer antimicrobial peptide, L1, which is also a venomous insect derived peptide like decoralin. These were used in comparison to the AP peptide which are host defense peptides.

In this study we investigated a several antimicrobial peptides and derivatives that had different sequence lengths and net charges. Decoralin (venom derived) and APX-12 (host defense derived) are two short antimicrobial peptides which exhibited different antimicrobial activity despite the similar length and net charge (Table 8). Although decoralin didn't exhibit the greatest antimicrobial activity of the peptides tested it did show greater activity than the truncated peptide APX-12. Considering the similarly in molecular weight and net charge (amino acid composition) this is an area of great interest of future study to determine the molecular rules that in part antimicrobial activity to a peptide sequence.

A similar approach was used when choosing and comparing the longer venom derived peptide L1 to the full length AP3 and derivatives. The L1 peptide is originally isolated from the venom of the predatory ant *Pachycondyla goeldii* and is a member of the subfamily of Ponerinae[98, 99]. Ponericin peptides are thought to exhibit a defensive role against microbial pathogens and are thought to adopt an amphipathic alpha-helical structure[98].

The results of initial characterization experiments of the two groups of peptides were compared. The data collected indicated that decoralin did bind to the model lipid membranes and, unlike APX peptides, exhibited a shift in significant shift in emission barycenter upon binding vesicles composed of 75%/25% POPC/POPG lipid composition.

As expected the decrease in anionic lipids (POPG in our study) showed a decrease in barycenter emission shift[70],[71],[72]. Although this is similar to other linear cationic peptides these results contrast with the results of the APX truncated peptides. Fluorescence quenching experiments for decoralin were found to be consistent with the truncated AP peptides, in that there was no significant difference in quenching between the bound and unbound samples. This indicates that these peptides adopt a shallowly oriented topography in the bilayer where the tryptophan remains significantly exposed to the aqueous environment. As expected, the results of CD spectra indicated decoralin adopted α-helical secondary structure in the presence of model lipid membranes. This was similar to the truncated APX peptides although the CD intensity was somewhat lower for the APX peptides. Bacterial membrane permeabilization (outer and inner membrane) and vesicle leakage assays showed moderate disruption compared to the AP full-length peptides but were greater than both APX truncated analogs.

Table 10

APX-12 and Decoralin Comparison

		Molecular Weight				**Percent Composition**		
Peptide	Sequence	Measured	Calculated	pI	Hydrophobic	Basic	Acidic	Neutral
APX-12	KTVGKLALKHWL	1393.7	1394.7	10.98	50%	33.33%	0%	16.67%
Decoralin	SLLSLWRKLIT	1327.5	1329.6	11.39	54.55%	18.18%	0%	27.27%

Our study demonstrated a potentially additive interaction of silver nitrate with either decoralin or L1. Identifying potential synergy between different antimicrobial species has become an area of great interest due to the ongoing problem with antibiotic resistance[4]. We chose silver nitrate because it is a broad spectrum antimicrobial like antimicrobial peptides but are thought to act by a different mechanism therefore the combination of the two could in theory have synergistic or additive effect. Our preliminary results of decoralin and L1 indicate a potential additive effect but it is still unclear if this effect can be categorized as synergistic. In future combinatorial experiments the fractional inhibitory concentration index (FICI) will be used to determine the degree of each combination of antimicrobials[93],[54]. FICI uses a combination of MICs for each antimicrobial species to determine whether the combination results in a synergistic, additive, or no effect. In future synergy studies we plan to use this method of testing and FICI to calculate the degree of synergy.

References

[1] O. Genilloud, "Current challenges in the discovery of novel antibacterials from microbial natural products," *Recent Pat Antiinfect Drug Discov,* vol. 7, pp. 189-204, Dec 1 2012.

[2] F. Pelaez, "The historical delivery of antibiotics from microbial natural products--can history repeat?," *Biochem Pharmacol,* vol. 71, pp. 981-90, Mar 30 2006.

[3] J. Clardy, M. A. Fischbach, and C. R. Currie, "The natural history of antibiotics," *Curr Biol,* vol. 19, pp. R437-41, Jun 9 2009.

[4] A. H. Holmes, L. S. Moore, A. Sundsfjord, M. Steinbakk, S. Regmi, A. Karkey*, et al.*, "Understanding the mechanisms and drivers of antimicrobial resistance," *Lancet,* vol. 387, pp. 176-87, Jan 9 2016.

[5] R. Laxminarayan, A. Duse, C. Wattal, A. K. Zaidi, H. F. Wertheim, N. Sumpradit*, et al.*, "Antibiotic resistance-the need for global solutions," *Lancet Infect Dis,* vol. 13, pp. 1057-98, Dec 2013.

[6] M. K. Rai, S. D. Deshmukh, A. P. Ingle, and A. K. Gade, "Silver nanoparticles: the powerful nanoweapon against multidrug-resistant bacteria," *J Appl Microbiol,* vol. 112, pp. 841-52, May 2012.

[7] M. L. Katz, L. V. Mueller, M. Polyakov, and S. F. Weinstock, "Where have all the antibiotic patents gone?," *Nat Biotech,* vol. 24, pp. 1529-1531, 12//print 2006.

[8] R. R. Watkins and R. A. Bonomo, "Overview: Global and Local Impact of Antibiotic Resistance," *Infect Dis Clin North Am,* vol. 30, pp. 313-22, Jun 2016.

[9] B. Khameneh, R. Diab, K. Ghazvini, and B. S. Fazly Bazzaz, "Breakthroughs in bacterial resistance mechanisms and the potential ways to combat them," *Microb Pathog,* vol. 95, pp. 32-42, Jun 2016.

[10] J. Carlet, C. Pulcini, and L. J. V. Piddock, "Antibiotic resistance: a geopolitical issue," *Clinical Microbiology and Infection,* vol. 20, pp. 949-953, 10// 2014.

[11] M. Baym, L. K. Stone, and R. Kishony, "Multidrug evolutionary strategies to reverse antibiotic resistance," *Science,* vol. 351, p. aad3292, Jan 1 2016.

[12] R. J. Worthington, J. J. Richards, and C. Melander, "Small molecule control of bacterial biofilms," *Org Biomol Chem,* vol. 10, pp. 7457-74, Oct 7 2012.

[13] G. Cheng, M. Dai, S. Ahmed, H. Hao, X. Wang, and Z. Yuan, "Antimicrobial Drugs in Fighting against Antimicrobial Resistance," *Front Microbiol,* vol. 7, p. 470, 2016.

[14] M. Moscoso, E. Garcia, and R. Lopez, "Pneumococcal biofilms," *Int Microbiol,* vol. 12, pp. 77-85, Jun 2009.

[15] N. M. Vandevelde, P. M. Tulkens, and F. Van Bambeke, "Modulating antibiotic activity towards respiratory bacterial pathogens by co-medications: a multi-target approach," *Drug Discov Today,* vol. 21, pp. 1114-29, Jul 2016.

[16] J. W. Alexander, "History of the medical use of silver," *Surg Infect (Larchmt),* vol. 10, pp. 289-92, Jun 2009.

[17] B. M. Geilich, A. L. van de Ven, G. L. Singleton, L. J. Sepulveda, S. Sridhar, and T. J. Webster, "Silver nanoparticle-embedded polymersome nanocarriers for the treatment of antibiotic-resistant infections," *Nanoscale,* vol. 7, pp. 3511-9, Feb 28 2015.

[18] S. L. Percival, J. Thomas, S. Linton, T. Okel, L. Corum, and W. Slone, "The antimicrobial efficacy of silver on antibiotic-resistant bacteria isolated from burn wounds," *Int Wound J,* vol. 9, pp. 488-93, Oct 2012.

[19] D. E. Marx and D. J. Barillo, "Silver in medicine: the basic science," *Burns,* vol. 40 Suppl 1, pp. S9-S18, Dec 2014.

[20] K. Mijnendonckx, N. Leys, J. Mahillon, S. Silver, and R. Van Houdt, "Antimicrobial silver: uses, toxicity and potential for resistance," *Biometals,* vol. 26, pp. 609-21, Aug 2013.

[21] S. Silver, "Bacterial silver resistance: molecular biology and uses and misuses of silver compounds," *FEMS Microbiol Rev,* vol. 27, pp. 341-53, Jun 2003.

[22] I. Chopra, "The increasing use of silver-based products as antimicrobial agents: a useful development or a cause for concern?," *J Antimicrob Chemother,* vol. 59, pp. 587-90, Apr 2007.

[23] K. Markowska, A. M. Grudniak, and K. I. Wolska, "Silver nanoparticles as an alternative strategy against bacterial biofilms," *Acta Biochim Pol,* vol. 60, pp. 523-30, 2013.

[24] R. Singh, U. U. Shedbalkar, S. A. Wadhwani, and B. A. Chopade, "Bacteriagenic silver nanoparticles: synthesis, mechanism, and applications," *Appl Microbiol Biotechnol,* vol. 99, pp. 4579-93, Jun 2015.

[25] N. Duran, M. Duran, M. B. de Jesus, A. B. Seabra, W. J. Favaro, and G. Nakazato, "Silver nanoparticles: A new view on mechanistic aspects on antimicrobial activity," *Nanomedicine,* vol. 12, pp. 789-99, Apr 2016.

[26] B. Mojsoska and H. Jenssen, "Peptides and Peptidomimetics for Antimicrobial Drug Design," *Pharmaceuticals (Basel),* vol. 8, pp. 366-415, 2015.

[27] R. E. Hancock, E. F. Haney, and E. E. Gill, "The immunology of host defence peptides: beyond antimicrobial activity," *Nat Rev Immunol,* vol. 16, pp. 321-34, May 2016.

[28] C. D. Sumi, B. W. Yang, I. C. Yeo, and Y. T. Hahm, "Antimicrobial peptides of the genus Bacillus: a new era for antibiotics," *Can J Microbiol,* vol. 61, pp. 93-103, Feb 2015.

[29] N. Y. Yount, A. S. Bayer, Y. Q. Xiong, and M. R. Yeaman, "Advances in antimicrobial peptide immunobiology," *Biopolymers,* vol. 84, pp. 435-58, 2006.

[30] N. Singh and J. Abraham, "Ribosomally synthesized peptides from natural sources," *J Antibiot (Tokyo),* vol. 67, pp. 277-89, Apr 2014.

[31] S. C. Mansour, O. M. Pena, and R. E. Hancock, "Host defense peptides: front-line immunomodulators," *Trends Immunol,* vol. 35, pp. 443-50, Sep 2014.

[32] M. Zasloff, "Antimicrobial peptides of multicellular organisms," *Nature,* vol. 415, pp. 389-95, Jan 24 2002.

[33] K. Konno, M. Rangel, J. S. Oliveira, M. P. Dos Santos Cabrera, R. Fontana, I. Y. Hirata*, et al.*, "Decoralin, a novel linear cationic alpha-helical peptide from the venom of the solitary eumenine wasp Oreumenes decoratus," *Peptides,* vol. 28, pp. 2320-7, Dec 2007.

[34] L. T. Nguyen, E. F. Haney, and H. J. Vogel, "The expanding scope of antimicrobial peptide structures and their modes of action," *Trends Biotechnol,* vol. 29, pp. 464-72, Sep 2011.

[35] C. D. Fjell, J. A. Hiss, R. E. Hancock, and G. Schneider, "Designing antimicrobial peptides: form follows function," *Nat Rev Drug Discov,* vol. 11, pp. 37-51, Jan 2012.

[36] Y. Li, Q. Xiang, Q. Zhang, Y. Huang, and Z. Su, "Overview on the recent study of antimicrobial peptides: origins, functions, relative mechanisms and application," *Peptides,* vol. 37, pp. 207-15, Oct 2012.

[37] A. Izadpanah and R. L. Gallo, "Antimicrobial peptides," *J Am Acad Dermatol,* vol. 52, pp. 381-90; quiz 391-2, Mar 2005.

[38] F. Azmi, A. G. Elliott, N. Marasini, S. Ramu, Z. Ziora, A. M. Kavanagh*, et al.*, "Short cationic lipopeptides as effective antibacterial agents: Design, physicochemical properties and biological evaluation," *Bioorg Med Chem,* vol. 24, pp. 2235-41, May 15 2016.

[39] J. P. Tam, S. Wang, K. H. Wong, and W. L. Tan, "Antimicrobial Peptides from Plants," *Pharmaceuticals (Basel),* vol. 8, pp. 711-57, 2015.

[40] H. Y. Yi, M. Chowdhury, Y. D. Huang, and X. Q. Yu, "Insect antimicrobial peptides and their applications," *Appl Microbiol Biotechnol,* vol. 98, pp. 5807-22, Jul 2014.

[41] J. M. Conlon, M. Mechkarska, and J. D. King, "Host-defense peptides in skin secretions of African clawed frogs (Xenopodinae, Pipidae)," *Gen Comp Endocrinol,* vol. 176, pp. 513-8, May 1 2012.

[42] Y. N. Antonenko, G. S. Gluhov, A. M. Firsov, I. D. Pogozheva, S. I. Kovalchuk, E. V. Pechnikova*, et al.*, "Gramicidin A disassembles large conductive clusters of its lysine-substituted derivatives in lipid membranes," *Phys Chem Chem Phys,* vol. 17, pp. 17461-70, Jul 14 2015.

[43] L. M. Gottler and A. Ramamoorthy, "Structure, membrane orientation, mechanism, and function of pexiganan--a highly potent antimicrobial peptide designed from magainin," *Biochim Biophys Acta,* vol. 1788, pp. 1680-6, Aug 2009.

[44] S. R. Aili, A. Touchard, P. Escoubas, M. P. Padula, J. Orivel, A. Dejean*, et al.*, "Diversity of peptide toxins from stinging ant venoms," *Toxicon,* vol. 92, pp. 166-78, Dec 15 2014.

[45] E. Jamasbi, A. Mularski, and F. Separovic, "Model Membrane and Cell Studies of Antimicrobial Activity of Melittin Analogues," *Curr Top Med Chem,* vol. 16, pp. 40-5, 2016.

[46] B. A. Costa, L. Sanches, A. B. Gomide, F. Bizerra, C. Dal Mas, E. B. Oliveira*, et al.*, "Interaction of the rattlesnake toxin crotamine with model membranes," *J Phys Chem B,* vol. 118, pp. 5471-9, May 22 2014.

[47] L. Kuhn-Nentwig, "Antimicrobial and cytolytic peptides of venomous arthropods," *Cell Mol Life Sci,* vol. 60, pp. 2651-68, Dec 2003.

[48] E. N. Worthington, I. H. Kavakli, G. Berrocal-Tito, B. E. Bondo, and A. Sancar, "Purification and characterization of three members of the photolyase/cryptochrome family blue-light photoreceptors from Vibrio cholerae," *J Biol Chem,* vol. 278, pp. 39143-54, Oct 3 2003.

[49] M. F. Tatner and M. T. Horne, "Susceptibility and immunity to Vibrio anguillarum in post-hatching rainbow trout fry, Salmo gairdneri Richardson 1836," *Dev Comp Immunol,* vol. 7, pp. 465-72, Summer 1983.

[50] P. Pundir, A. Catalli, C. Leggiadro, S. E. Douglas, and M. Kulka, "Pleurocidin, a novel antimicrobial peptide, induces human mast cell activation through the FPRL1 receptor," *Mucosal Immunol,* vol. 7, pp. 177-87, Jan 2014.

[51] A. M. Cole, P. Weis, and G. Diamond, "Isolation and characterization of pleurocidin, an antimicrobial peptide in the skin secretions of winter flounder," *J Biol Chem,* vol. 272, pp. 12008-13, May 2 1997.

[52] G. Yu, D. Y. Baeder, R. R. Regoes, and J. Rolff, "Combination Effects of Antimicrobial Peptides," *Antimicrob Agents Chemother,* vol. 60, pp. 1717-24, Mar 2016.

[53] W. R. Greco, H. Faessel, and L. Levasseur, "The search for cytotoxic synergy between anticancer agents: a case of Dorothy and the ruby slippers?," *J Natl Cancer Inst,* vol. 88, pp. 699-700, Jun 5 1996.

[54] H. Choi and D. G. Lee, "Synergistic effect of antimicrobial peptide arenicin-1 in combination with antibiotics against pathogenic bacteria," *Res Microbiol,* vol. 163, pp. 479-86, Jul 2012.

[55] (2016). *How we die (by the numbers)*. Available: http://www.cnn.com/2016/06/02/health/gallery/how-we-die/index.html

[56] Available: https://marine.rutgers.edu/navesink/about.htm

[57] Z. Ridgway, A. L. Picciano, P. M. Gosavi, Y. S. Moroz, C. E. Angevine, A. E. Chavis*, et al.*, "Functional characterization of a melittin analog containing a non-natural tryptophan analog," *Biopolymers,* vol. 104, pp. 384-94, Jul 2015.

[58] G. A. Caputo and E. London, "Using a novel dual fluorescence quenching assay for measurement of tryptophan depth within lipid bilayers to determine hydrophobic alpha-helix locations within membranes," *Biochemistry,* vol. 42, pp. 3265-74, Mar 25 2003.

[59] L. G. Burman, K. Nordstrom, and H. G. Boman, "Resistance of Escherichia coli to penicillins. V. Physiological comparison of two isogenic strains, one with chromosomally and one with episomally mediated ampicillin resistance," *J Bacteriol,* vol. 96, pp. 438-46, Aug 1968.

[60] I. Wiegand, K. Hilpert, and R. E. Hancock, "Agar and broth dilution methods to determine the minimal inhibitory concentration (MIC) of antimicrobial substances," *Nat Protoc,* vol. 3, pp. 163-75, 2008.

[61] J. Lee, S. W. Jung, and A. E. Cho, "Molecular Insights into the Adsorption Mechanism of Human beta-Defensin-3 on Bacterial Membranes," *Langmuir,* vol. 32, pp. 1782-90, Feb 23 2016.

[62] T. D. Clark, L. Bartolotti, and R. P. Hicks, "The application of DOSY NMR and molecular dynamics simulations to explore the mechanism(s) of micelle binding of antimicrobial peptides containing unnatural amino acids," *Biopolymers,* vol. 99, pp. 548-61, Aug 2013.

[63] G. A. Caputo and E. London, "Cumulative effects of amino acid substitutions and hydrophobic mismatch upon the transmembrane stability and conformation of hydrophobic alpha-helices," *Biochemistry,* vol. 42, pp. 3275-85, Mar 25 2003.

[64] V. V. Andrushchenko, M. H. Aarabi, L. T. Nguyen, E. J. Prenner, and H. J. Vogel, "Thermodynamics of the interactions of tryptophan-rich cathelicidin antimicrobial peptides with model and natural membranes," *Biochim Biophys Acta,* vol. 1778, pp. 1004-14, Apr 2008.

[65] V. P. Nguyen, D. S. Alves, H. L. Scott, F. L. Davis, and F. N. Barrera, "A Novel Soluble Peptide with pH-Responsive Membrane Insertion," *Biochemistry,* vol. 54, pp. 6567-75, Nov 3 2015.

[66] B. Mensa, Y. H. Kim, S. Choi, R. Scott, G. A. Caputo, and W. F. DeGrado, "Antibacterial mechanism of action of arylamide foldamers," *Antimicrob Agents Chemother,* vol. 55, pp. 5043-53, Nov 2011.

[67] Y. Jin, L. X. Duan, X. L. Xu, W. J. Ge, R. F. Li, X. J. Qiu*, et al.*, "Mechanism of apoptosis induction in human hepatocellular carcinoma cells following treatment with a gecko peptides mixture," *Biomed Rep,* vol. 5, pp. 73-78, Jul 2016.

[68] C. Y. Yeh, J. K. Hsiao, Y. P. Wang, C. H. Lan, and H. C. Wu, "Peptide-conjugated nanoparticles for targeted imaging and therapy of prostate cancer," *Biomaterials,* vol. 99, pp. 1-15, Aug 2016.

[69] R. Izabela, R. Jaroslaw, A. Magdalena, R. Piotr, and K. Ivan, "Transportan 10 improves the anticancer activity of cisplatin," *Naunyn Schmiedebergs Arch Pharmacol,* vol. 389, pp. 485-97, May 2016.

[70] G. Batoni, M. Casu, A. Giuliani, V. Luca, G. Maisetta, M. L. Mangoni*, et al.*, "Rational modification of a dendrimeric peptide with antimicrobial activity: consequences on membrane-binding and biological properties," *Amino Acids,* vol. 48, pp. 887-900, Mar 2016.

[71] V. Teixeira, M. J. Feio, and M. Bastos, "Role of lipids in the interaction of antimicrobial peptides with membranes," *Prog Lipid Res,* vol. 51, pp. 149-77, Apr 2012.

[72] I. D. Alves, I. Correia, C. Y. Jiao, E. Sachon, S. Sagan, S. Lavielle*, et al.*, "The interaction of cell-penetrating peptides with lipid model systems and subsequent lipid reorganization: thermodynamic and structural characterization," *J Pept Sci,* vol. 15, pp. 200-9, Mar 2009.

[73] S. Bandyopadhyay, M. Lee, J. Sivaraman, and C. Chatterjee, "Model membrane interaction and DNA-binding of antimicrobial peptide Lasioglossin II derived from bee venom," *Biochem Biophys Res Commun,* vol. 430, pp. 1-6, Jan 4 2013.

[74] C. Monteiro, M. Pinheiro, M. Fernandes, S. Maia, C. L. Seabra, F. Ferreira-da-Silva*, et al.*, "A 17-mer Membrane-Active MSI-78 Derivative with Improved Selectivity toward Bacterial Cells," *Mol Pharm,* vol. 12, pp. 2904-11, Aug 3 2015.

[75] D. J. Hirst, T. H. Lee, K. Kulkarni, J. A. Wilce, and M. I. Aguilar, "The impact of cell-penetrating peptides on membrane bilayer structure during binding and insertion," *Biochim Biophys Acta,* vol. 1858, pp. 1841-9, Aug 2016.

[76] K. Lohner, "New strategies for novel antibiotics: peptides targeting bacterial cell membranes," *Gen Physiol Biophys,* vol. 28, pp. 105-16, Jun 2009.

[77] A. Therrien, A. Fournier, and M. Lafleur, "Role of the Cationic C-Terminal Segment of Melittin on Membrane Fragmentation," *J Phys Chem B,* vol. 120, pp. 3993-4002, May 5 2016.

[78] A. Tossi, L. Sandri, and A. Giangaspero, "Amphipathic, alpha-helical antimicrobial peptides," *Biopolymers,* vol. 55, pp. 4-30, 2000.

[79] U. Baul, K. Kuroda, and S. Vemparala, "Interaction of multiple biomimetic antimicrobial polymers with model bacterial membranes," *J Chem Phys,* vol. 141, p. 084902, Aug 28 2014.

[80] I. Ivanov, S. Vemparala, V. Pophristic, K. Kuroda, W. F. DeGrado, J. A. McCammon*, et al.*, "Characterization of nonbiological antimicrobial polymers in aqueous solution and at water-lipid interfaces from all-atom molecular dynamics," *J Am Chem Soc,* vol. 128, pp. 1778-9, Feb 15 2006.

[81] M. L. Juba, D. K. Porter, E. H. Williams, C. A. Rodriguez, S. M. Barksdale, and B. M. Bishop, "Helical cationic antimicrobial peptide length and its impact on membrane disruption," *Biochim Biophys Acta,* vol. 1848, pp. 1081-91, May 2015.

[82] N. Takei, N. Takahashi, T. Takayanagi, A. Ikeda, K. Hashimoto, M. Takagi*, et al.*, "Antimicrobial activity and mechanism of action of a novel cationic alpha-helical dodecapeptide, a partial sequence of cyanate lyase from rice," *Peptides,* vol. 42, pp. 55-62, Apr 2013.

[83] E. K. Lee, Y. C. Kim, Y. H. Nan, and S. Y. Shin, "Cell selectivity, mechanism of action and LPS-neutralizing activity of bovine myeloid antimicrobial peptide-18 (BMAP-18) and its analogs," *Peptides,* vol. 32, pp. 1123-30, Jun 2011.

[84] K. Lohner and E. J. Prenner, "Differential scanning calorimetry and X-ray diffraction studies of the specificity of the interaction of antimicrobial peptides with membrane-mimetic systems," *Biochim Biophys Acta,* vol. 1462, pp. 141-56, Dec 15 1999.

[85] W. Dong, Z. Dong, X. Mao, Y. Sun, F. Li, and D. Shang, "Structure-activity analysis and biological studies of chensinin-1b analogues," *Acta Biomater,* vol. 37, pp. 59-68, Jun 2016.

[86] B. Mathew and R. Nagaraj, "Antimicrobial activity of human alpha-defensin 6 analogs: insights into the physico-chemical reasons behind weak bactericidal activity of HD6 in vitro," *J Pept Sci,* vol. 21, pp. 811-8, Nov 2015.

[87] J. S. Bahnsen, H. Franzyk, A. Sandberg-Schaal, and H. M. Nielsen, "Antimicrobial and cell-penetrating properties of penetratin analogs: effect of sequence and secondary structure," *Biochim Biophys Acta,* vol. 1828, pp. 223-32, Feb 2013.

[88] R. Fontana, M. A. Mendes, B. M. de Souza, K. Konno, L. M. Cesar, O. Malaspina*, et al.*, "Jelleines: a family of antimicrobial peptides from the Royal Jelly of honeybees (Apis mellifera)," *Peptides,* vol. 25, pp. 919-28, Jun 2004.

[89] X. Hou, Q. Du, R. Li, M. Zhou, H. Wang, L. Wang*, et al.*, "Feleucin-BO1: a novel antimicrobial non-apeptide amide from the skin secretion of the toad, Bombina orientalis, and design of a potent broad-spectrum synthetic analogue, feleucin-K3," *Chem Biol Drug Des,* vol. 85, pp. 259-67, Mar 2015.

[90] T. N. Demidova and M. R. Hamblin, "Effect of cell-photosensitizer binding and cell density on microbial photoinactivation," *Antimicrob Agents Chemother,* vol. 49, pp. 2329-35, Jun 2005.

[91] H. H. Wang, F. J. Isaacs, P. A. Carr, Z. Z. Sun, G. Xu, C. R. Forest*, et al.*, "Programming cells by multiplex genome engineering and accelerated evolution," *Nature,* vol. 460, pp. 894-8, Aug 13 2009.

[92] J. N. Anderl, M. J. Franklin, and P. S. Stewart, "Role of antibiotic penetration limitation in Klebsiella pneumoniae biofilm resistance to ampicillin and ciprofloxacin," *Antimicrob Agents Chemother,* vol. 44, pp. 1818-24, Jul 2000.

[93] M. M. Sopirala, J. E. Mangino, W. A. Gebreyes, B. Biller, T. Bannerman, J. M. Balada-Llasat*, et al.*, "Synergy testing by Etest, microdilution checkerboard, and time-kill methods for pan-drug-resistant Acinetobacter baumannii," *Antimicrob Agents Chemother,* vol. 54, pp. 4678-83, Nov 2010.

[94] R. K. Shields, E. J. Kwak, B. A. Potoski, Y. Doi, J. M. Adams-Haduch, F. P. Silviera*, et al.*, "High mortality rates among solid organ transplant recipients infected with extensively drug-resistant Acinetobacter baumannii: using in vitro antibiotic combination testing to identify the combination of a carbapenem and colistin as an effective treatment regimen," *Diagn Microbiol Infect Dis,* vol. 70, pp. 246-52, Jun 2011.

[95] C. S. Cavalcante, C. B. Falcao, R. O. Fontenelle, D. Andreu, and G. Radis-Baptista, "Anti-fungal activity of Ctn[15-34], the C-terminal peptide fragment of crotalicidin, a rattlesnake venom gland cathelicidin," *J Antibiot (Tokyo),* Nov 23 2016.

[96] M. Berditsch, T. Jager, N. Strempel, T. Schwartz, J. Overhage, and A. S. Ulrich, "Synergistic effect of membrane-active peptides polymyxin B and gramicidin S on multidrug-resistant strains and biofilms of Pseudomonas aeruginosa," *Antimicrob Agents Chemother,* vol. 59, pp. 5288-96, Sep 2015.

[97] V. Aleksic, N. Mimica-Dukic, N. Simin, N. S. Nedeljkovic, and P. Knezevic, "Synergistic effect of Myrtus communis L. essential oils and conventional antibiotics against multi-drug resistant Acinetobacter baumannii wound isolates," *Phytomedicine,* vol. 21, pp. 1666-74, Oct 15 2014.

[98] J. Orivel, V. Redeker, J. P. Le Caer, F. Krier, A. M. Revol-Junelles, A. Longeon*, et al.*, "Ponericins, new antibacterial and insecticidal peptides from the venom of the ant Pachycondyla goeldii," *J Biol Chem,* vol. 276, pp. 17823-9, May 25 2001.

[99] Y. F. Chen, P. W. Sun, and D. Z. Tang, "[Antimicrobial activities of ant Ponericin W1 against plant pathogens in vitro and the disease resistance in its transgenic Arabidopsis]," *Yi Chuan,* vol. 35, pp. 1023-9, Aug 2013.